POLYTECHNIQUE MONTRÉAL

affiliée à l'Université de Montréal

Role of MgO in the remineralization and removal of manganese in drinking water

LENA SZYMONIAK

Département de Génie Civil

Mémoire

présenté en vue de l'obtention du diplôme de *Maîtrise ès sciences appliquées*

Génie Civil

Avril 2021

© Lena Szymoniak, 2021.

POLYTECHNIQUE MONTRÉAL

affiliée à l'Université de Montréal

Ce mémoire intitulé:

Role of MgO in the remineralization and removal of manganese in drinking water

présenté par

Lena SZYMONIAK

en vue de l'obtention du diplôme de *Maîtrise ès sciences appliquées*

a été dûment accepté par le jury d'examen constitué de :

Yves COMEAU, président
Benoit BARBEAU, membre et directeur
Dominique CLAVEAU-MALLET, membre et codirectrice de recherche
Maryam HADDAD, membre et codirectrice de recherche
Benoît COURCELLES, membre

ACKNOWLEDGEMENTS

I would like to acknowledge the many people that it took for this work to come together. Thank you first and foremost to the wonderful technicians and research associates at CREDEAU laboratory. Mireille, Yves, Tetiana, Julie, Jacinthe and Gabriel- without you I would most certainly still be titrating my days away.

Thank you, Laura, for helping everything run smoothly as well. We don't always see the administrative side of things in the lab, but you tie all the threads together!

Thank you especially to Benoit, Dominique and Maryam, for the guidance, the discussions and the support that you have offered- I count myself as very lucky to have had you as supervisors. This project has allowed me to challenge myself and I am glad to have had the opportunity to do so in your company.

I would also like to acknowledge the members of my committee, Professor Yves Comeau and Professor Benoît Courcelles for taking interest in my work and examining my thesis.

Much appreciation also goes to the other members of our research team and the peers encountered during my time at Polytechnique, it has been a pleasure exchanging ideas and getting to know you all. I look forward to following your projects in the future!

RÉSUMÉ

Le manganèse (Mn) est l'un des métaux les plus abondants dans la croûte terrestre. Dans les eaux souterraines, les taux de détection varient en fonction de la composition chimique des précipitations, du type de matériaux de l'aquifère, des différences dans les temps de résidence des eaux, et des conditions rédox dans l'aquifère. En général, les conditions anaérobies sont dominantes dans les eaux souterraines, ce qui peut entraîner des niveaux élevés de manganèse dissous. La réglementation concernant les concentrations de Mn dans l'eau potable est un sujet de préoccupation récent. Bien qu'il soit considéré comme un micro-nutriment essentiel au fonctionnement de nombreuses enzymes cellulaires, une surexposition au Mn peut causer des effets néfastes sur la santé. En particulier, il existe de plus en plus de preuves de la neurotoxicité de cet élément. Les données canadiennes font généralement état de valeurs inférieures à 100 µg/L de Mn dans l'eau du robinet, mais dans certains cas les niveaux atteignent des milliers de microgrammes par litre. La consommation quotidienne d'eau minérale a donc le potentiel de contribuer de manière significative à l'apport en manganèse. En outre, les problèmes esthétiques et opérationnels causés par une teneur élevée en Mn font en sorte que le traitement de ce métal est bien établi. À partir de 20 µg/L, la présence de manganèse a déjà donné lieu à des plaintes de consommateurs concernant la décoloration de l'eau, la coloration des appareils sanitaires et des tissus. Sur la base des informations ci-dessus et des conditions des eaux souterraines au Canada, Santé Canada a mis à jour la concentration maximale acceptable de Mn dans l'eau potable à 120 µg/L et l'objectif esthétique à 20 µg/L. Les traitements du Mn au niveau résidentiel comprennent généralement des technologies de filtration catalytique ou d'échange de cations couplées à l'osmose inversée au point d'utilisation. Ce travail de maîtrise étudie la capacité d'un contacteur au media mixte composé de calcite ($CaCO_3$) et d'oxyde de magnésium (MgO) comme étape de polissage après un processus alternatif d'élimination du Mn utilisant une membrane de nanofiltration à fibres creuses (HFNF). L'utilisation de MgO est particulièrement intéressante car, bien que ce media ne soit pas nouveau dans l'industrie du traitement de l'eau, peu de travaux concernent son application dans le contexte de l'eau potable. Cependant, une revue de la littérature a révélé que l'hydratation rapide du MgO et la faible solubilité du $Mg(OH)_2$ fournissent une source d'alcalinité et de Mg^{2+} (un cation considéré bénéfique pour la santé humaine) à long terme. La dissolution du media occasionne aussi une gamme de pH propice à la précipitation des métaux divalents tels que le Mn^{2+}. L'objectif principal

était donc d'étudier la contribution de MgO dans le processus de reminéralisation et d'élimination du Mn d'un contacteur de calcite. Les objectifs spécifiques ont été définis comme suit : 1) étudier l'effet du rapport $CaCO_3$/MgO sur la cinétique de dissolution du media dans un filtre mixte ; 2) comparer la cinétique d'élimination du Mn en utilisant du $CaCO_3$ et du MgO frais et usagé ; 3) déterminer l'importance relative de la sorption par rapport à la précipitation dans l'élimination du Mn par le MgO ; 4) évaluer l'effet des noyaux de précipitation sur la cinétique d'élimination du Mn.

Le projet comprenait deux phases expérimentales : 1) des expériences continues de sorption-dissolution (en colonne) à l'échelle pilote et 2) des expériences d'essai en batch pour étudier l'effet de la charge en Mn sur l'élimination subséquente du Mn dissous. Dans la première phase, deux concentrations initiales de Mn (0.5 et 5 mg Mn/L) ont été traitées pendant 72 heures avec des colonnes contenant des fractions croissantes de MgO (0-20%). L'ajout d'une dureté de 30 mg $CaCO_3$/L et l'élimination du Mn en dessous de l'objectif esthétique (20 µg/L) ont été visés à l'effluent. Alors que tous les ratios ont permis d'atteindre la qualité d'eau ciblée, l'ajout de 10 et 20 % de MgO a provoqué une "sur-correction" du pH à plus de 10.5. Par conséquent, l'opération à long terme de la colonne de media mixte (720 heures) a été effectuée avec 5% de MgO. La réduction de la teneur en MgO a permis de limiter le pH à 10.5 et moins, tout en atteignant les objectifs de reminéralisation et d'élimination du Mn pour la durée de l'expérience. L'analyse de media usagés par spectroscopie photo-électronique à rayons-X a identifié jusqu'à 10% d'oxydes de Mn (MnO_x) sur les surfaces de MgO et près de 1.5% sur celles des grains de $CaCO_3$. La deuxième phase expérimentale a permis d'étudier la cinétique d'élimination du Mn en utilisant le media chargé en Mn issus des premiers essais en colonne (72h d'opération). Sur 48 heures, les essais en batch ont montré que la calcite fraîche et chargée en Mn (5 mg Mn/g d'échantillon) nécessitait plus de temps pour atteindre un régime de sorption stable en comparaison avec le MgO frais ou les medias mixtes chargés en Mn (5 mg Mn/g d'échantillon) qui se sont stabilisés en une heure. De même, les régimes de sorption des medias chargés en Mn (0-10% MgO) ont convergés autour d'un taux élimination de 76% du Mn après 8 heures. Nous avons émis l'hypothèse que si l'augmentation de la fraction de MgO accélère la cinétique initiale d'élimination du Mn, la charge de Mn sur les surfaces de medias usagés reste probablement un facteur important dans l'élimination continue du Mn pendant l'opération de la colonne. Les résultats des essais en batch ont également suggéré que

la précipitation induite par le pH est un mécanisme important dans la réaction d'élimination du Mn qui se produit dans un contacteur à media mixte avec aussi peu que 5% de MgO. Par conséquent, une étape de précipitation pourrait expliquer l'augmentation du taux d'élimination observée par rapport à la calcite pure, chargé à la même concentration de Mn. Il a été conclu que la dissolution de MgO provoque possiblement la précipitation d'une fraction de la phase aqueuse de Mn sous forme d'hydroxydes et de carbonates de Mn en raison du pH élevé de la solution. De plus, la sorption sur ces phases solides de Mn contrôle la cinétique d'élimination une fois que les noyaux de précipitation sont établis et que la phase aqueuse est considérablement réduite.

ABSTRACT

Manganese (Mn) is one of the most abundant metals in Earth's crust, and in groundwater (GW), detection rates vary in relation to rainfall chemistry, the type of aquifer materials, differences in GW residence times, and redox conditions in the aquifer. In general, anaerobic conditions are dominant in groundwater, which can cause elevated levels of dissolved manganese. Regulation of Mn concentrations in drinking water has been a recent topic of concern. While it is considered a micro-nutrient essential to the proper functioning of many cellular enzymes, adverse health effects can be caused by an overexposure of Mn. In particular, there is increased evidence of the neurotoxicity of the element. Canadian data typically reports values under 100 µg/L of Mn in tap water, however there are cases where levels may reach thousands of micrograms per liter. Drinking mineral water regularly therefore has the potential to add significantly to manganese intake. In addition, aesthetic and operational issues caused by high Mn content make the efficient removal of the metal from drinking water a common concern. At concentrations exceeding 20 µg/L, the presence of manganese has led to consumer complaints about water discoloration and staining of fixtures and laundry. Based on the above information and the GW conditions in Canada, Health Canada has updated the maximum acceptable concentration (MAC) of Mn in drinking water to 120 µg/L and the aesthetic objective (AO) to 20 µg/L. Residential scale treatments of Mn in GW commonly include catalytic filtration or cation exchange (IX) technologies coupled with point of use reverse osmosis. This Master's work investigates the operational capacity of a mixed media contactor using calcite ($CaCO_3$) and magnesium oxide (MgO) as a polishing step following an alternative Mn removal process using a non-selective hollow fiber nanofiltration (HFNF) membrane. The use of MgO is of particular interest because although the media is not novel to the water treatment industry, there is surprisingly little work available regarding its application in the drinking water context. However, a review of the literature revealed that the quick hydration of the media and low solubility of $Mg(OH)_2$ provides a long-term source of alkalinity and Mg^{2+} (a cation considered beneficial to human health), and its dissolution provides a pH buffering range conducive to the precipitation of divalent metals such as Mn^{2+}. The main objective was therefore to investigate the contribution of MgO in the remineralization and Mn removal process of a calcite contactor. The specific objectives were defined as follows : 1) study the effect of the $CaCO_3$/MgO ratio on the dissolution kinetics of media in a mixed filter; 2) compare the Mn removal kinetics of fresh and

used $CaCO_3$ and MgO; 3) determine the relative importance of sorption vs. precipitation in Mn removal by MgO; 4) evaluate the effect of precipitation nuclei on the removal kinetics of Mn.

The project included two experimental phases: 1) continuous sorption-dissolution column experiments at the pilot-scale and 2) batch test experiments investigating the effect of Mn-loading on subsequent Mn removal. In the first phase, two initial concentrations of Mn (0.5 and 5 mg Mn/L) were treated over 72 hours with columns containing increasing MgO fractions (0-20%). The target water quality was the addition of hardness as 30 mg $CaCO_3$/L and the removal of Mn below the AO (20 μg/L) at the effluent. While all ratios were able to produce a treated water with target water quality, the addition of both 10 and 20% MgO caused the 'over-correction' of pH to above 10.5. Therefore, long-term operation of the mixed media column (720 hour) was performed with 5% MgO. Reducing the MgO content successfully constrained the pH to 10.5 and below, while achieving remineralization and Mn removal targets for the duration of the experiment. X-ray photoelectron spectroscopy (XPS) analysis of used media sampled from the entrance of the column treating 5 mg Mn/L identified up to 10% Mn oxides (MnO_x) on MgO surfaces and closer to1.5% on those of $CaCO_3$ media. The second experimental phase consequently investigated Mn removal kinetics using Mn-loaded media from the initial week-long column tests. Over 48 hours, batch tests showed that fresh and Mn-loaded calcite (5 mg Mn/g sample) required longer time to attain a stable sorption regime in comparison to fresh MgO or Mn-loaded mixed media (5 mg Mn/g sample) which stabilized within an hour. As well, the sorption regime of Mn-loaded media (0-10% MgO), converged at 76% Mn removal after 8 hours. It was hypothesized that while increasing the MgO fraction accelerates initial Mn-removal kinetics, the formation of Mn-phases seeds on the used media surfaces likely remains an important factor in continued Mn- removal during the operation of the column. Batch test results also suggested that pH-induced precipitation is an important mechanism in the Mn-removal reaction occurring in a mixed media contactor with as little as 5% MgO. Therefore, a precipitation step could account for the increased rate of removal which is seen in comparison to pure calcite with the same concentration of solid Mn-phase. It was concluded that the dissolution of MgO likely causes the precipitation of a fraction of the aqueous Mn-phase as Mn hydroxides and carbonates due to high solution pH, while solid Mn-phase sorption controls removal kinetics once precipitation nuclei are established and the aqueous phase has been significantly reduced.

TABLE OF CONTENTS

ACKNOWLEDGEMENTS III

RÉSUMÉ IV

ABSTRACT VII

TABLE OF CONTENTS IX

LIST OF TABLES XII

LIST OF FIGURES XIII

LIST OF SYMBOLS AND ABBREVIATIONS XV

LIST OF APPENDICES XVIII

CHAPTER 1 INTRODUCTION 1

1.1 Background 1

1.1 Structure of thesis 2

CHAPTER 2 ARTICLE 1 - APPLICATION OF MAGNESIUM OXIDE MEDIA FOR REMINERALIZATION AND CONTAMINANT REMOVAL IN DRINKING WATER TREATMENT: A REVIEW 4

2.1 Background and objectives 5

2.2 Magnesium oxide sources and properties 7

2.3 Mechanisms in MgO dissolution 8

2.4 Parameters affecting MgO dissolution in water treatment 11

2.4.1 Media Impurities 12

2.4.2 Particle Size and Shape 12

2.4.3 Internal Particle Porosity 12

2.4.4 Feed water composition 13

2.5 Comparison to calcite dissolution 19

2.6 Water treatment applications 19
2.6.1 Main applications 20
2.6.2 Scale formation 23
2.6.3 Issues with media coating 24
2.6.4 Process design and process control by modelling 25
2.6.5 Costs 28
2.7 Discussion and suggestions for further research 28
2.8 Conclusion 30
CHAPTER 3 RESEARCH OBJECTIVES, HYPOTHESES AND METHODOLOGY 31
3.1 Objectives and hypotheses 31
3.1.1 General objective 31
3.1.2 Specific objectives 31
3.1.3 Research hypotheses 31
3.2 Methodology 31
3.2.1 Continuous sorption-dissolution column experiments with mixed media 32
3.2.2 Batch sorption experiments on Mn-loaded media 36
CHAPTER 4 RESULTS 37
4.1 Continuous sorption-dissolution experiments 37
4.1.1 Impact of MgO ratio 37
4.1.2 Impact of influent Mn concentration 41
4.1.3 Impact of EBCT 41
4.1.4 Impact of operation time: 30-day experiment 42
4.2 Media Characterization 46
4.3 Batch sorption experiments on Mn-loaded media 49

4.3.1 Mn removal kinetics 49

4.3.2 Effect of pH on precipitation of $Mn_{(aq)}$ 51

4.3.3 Effect of precipitation nuclei on Mn sorption 51

CHAPTER 5 GENERAL DISCUSSION 53

5.1 Impact of MgO ratio on Mn removal and hardness adjustment 53

5.2 Mn removal kinetics using fresh and used $CaCO_3$ and MgO 54

5.3 Importance of sorption vs. precipitation in Mn removal by MgO 54

5.4 The effect of precipitation nuclei on the removal kinetics of Mn 55

5.5 Modeling the long-term performance of a mixed media contactor for Mn-removal and remineralization 56

CHAPTER 6 CONCLUSIONS AND RECOMMENDATIONS 57

REFERENCES 59

APPENDIX A MEDIA CHARACTERIZATION 69

LIST OF TABLES

Table 2.1 Solubility products at 25°C and 1 bar total pressure. 9

Table 2.2 Models of MgO in water treatment applications. 27

Table 3.1 Characteristics of $CaCO_3$ and MgO used in the study. 33

Table 3.2 Volume of buffer required to increase solution to target pH. 36

Table 4.1 High resolution XPS spectra for fresh and Mn-loaded media. 48

LIST OF FIGURES

Figure 2.1 Effect of calcination temperature on the morphology of an MgO aggregate. Image (a) shows 1 hour of calcination at 900 °C and (b) at 1100 °C. According to the authors, specific surface area decreased by a factor of 13 for the sample calcined at only 200 °C higher. 7

Figure 2.2 A) Theoretical solubility curves for pure $CaCO_3$ or MgO, in open (dotted) and closed (solid) systems. Before entering the batch simulation, the influent has zero Ca^{2+} or Mg^{2+} hardness and is prepared at varying pH by the addition of HCl or NaOH. B) Corresponding effluent pH following the dissolution of each media. 16

Figure 2.3 Comparative summary of MgO and $CaCO_3$ remineralization in soft water containing dissolved divalent metals. The thickness of the dashed arrows indicates relative reaction kinetics, and the presence of CO_2 increases the dissolution of the two media and the MgO hydration product, $Mg(OH)_2$. The main reactions in each system are as follows: 1) rapid hydration of MgO into Mg $(OH)_2$, and 2) removal of Me^{2+} by oxidation and sorption-coprecipitation process or possible cation exchange. In a $CaCO_3$ system the Me^{2+} is removed by 3) ionic exchange, followed by 4) the slow recrystallization of $MeCO_3$ to MeO_2. 21

Figure 3.1 Grainsize distribution curves for $CaCO_3$ and MgO media. 32

Figure 3.2 Schematic of laboratory column installation. 34

Figure 4.1 Figure 4.3 Evolution of pH, alkalinity and DIC over 72 hours (23 ± 2 °C). Samples were taken at 20 cm column depth (5 min EBCT) and at the effluent (20 min EBCT).....38

Figure 4.2 Evolution of A) total hardness addition and B) calcium and magnesium hardness contribution at the effluent over 72 hours (23 ± 2 °C). Samples were taken at 20 cm column depth (5 min EBCT) and at the effluent (20 min EBCT). 39

Figure 4.3 Manganese removal in 72-hour column experiments (23 ± 2 °C). Samples were taken at 20 cm column depth (5 min EBCT) and at the effluent (20 min EBCT). 40

Figure 4.4 Evolution of pH, alkalinity and DIC over 720-hour column experiments using a 95/5 ratio of $CaCO_3$/MgO (23 ± 2 °C). Samples were taken at 20 cm column depth (5 min EBCT) and at the effluent (20 min EBCT). 43

Figure 4.5 Evolution of A) total hardness addition and B) calcium and magnesium hardness contribution at the effluent in the 720-hour column experiments using a 95/5 ratio of $CaCO_3$/MgO (23 ± 2 °C). Samples were taken at 20 cm column depth (5 min EBCT) and at the effluent (20 min EBCT). 44

Figure 4.6 Manganese removal in 720-hour column experiments using a 95/5 ratio of $CaCO_3$/MgO (23 ± 2 °C). Samples were taken at 20 cm column depth (5 min EBCT) and at the effluent (20 min EBCT).....45

Figure 4.7 SEM images (x 1000 magnification) of Mn-loaded media surfaces. 47

Figure 4.8 XPS analysis of Mn-loaded (15 mg/g sample) MgO in blue and $CaCO_3$ in red for the region of Mn oxides. 49

Figure 4.9 A) Impact of solid Mn-phase (5 mg Mn/ g sample) and media ratio on Mn^{2+} removal in batch tests, B) impact of pH evolution (labelled points) leading to stable Mn-removal regimes and C) pH-induced precipitation of Mn in the absence of media (23 ± 2 °C). 50

Figure A.1 A) Mixed media columns containing 5% MgO after 720 hours of operation, B) fresh MgO and $CaCO_3$ and C) used media samples taken from column B after treating 5 mg Mn/L for 30 days. The red circle shows MgO grains that do not appear to be covered in with solid Mn-phase (MnO_x). 68

LIST OF SYMBOLS AND ABBREVIATIONS

Al	Aluminum
AMD	Acid Mine Drainage
ANSI	American National Standards Institute
AO	Aesthetic Objective
BE	Binding Energy
BET	Brunauer-Emmett-Teller
BNG	Boundary Nucleation and Growth
$CaCl_2$	Calcium Chloride
$CaCO_3$	Calcium Carbonate
CaO	Lime
Cd	Cadmium
Co	Cobalt
CO_2	Carbon Dioxide
Cu	Copper
D_{10}	Effective Grain Size
D_{50}	Median Grain Size
DIC	Dissolved Inorganic Carbon
DO	Dissolved Oxygen
E	Reaction Activation Energy
EBCT	Empty Bed Contact Time
EDX	Energy Dispersive X-ray
Fe	Iron
GW	Groundwater

H_2SO_4	Sulfuric Acid
HFNF	Hollow Fiber Nanofiltration
IAP	Ion Activity Product
ICP-MS	Inductively Coupled Plasma Mass Spectrometry
ICP-OES	Inductively Coupled Plasma Optical Emission Spectrometry
IX	Ion Exchange
JMAK	Johnson & Mehl, Avrami and Kolmogorov
K	Solubility Constant
MAC	Maximum Acceptable Concentration
Me^{2+}	Divalent Metal
$Mg(OH)_2$	Magnesium Hydroxide or Brucite
$MgCl_2$	Magnesium Chloride
$MgCO_3$	Magnesite
MgO	Magnesium Oxide
Mn	Manganese
MnO_x	Manganese Oxide
$MnSO_4$	Manganese Sulfate
Na_2CO_3	Sodium Carbonate
Ni	Nickel
NSF	NSF International
ORP	Oxidation-Reduction Potential
Pb	Lead
pH_{eq}	Saturation pH
POE	Point of Entry

PWP	Plummer, Parkhurst and Wigley Model
R	Universal Gas Constant
RO	Reverse Osmosis
SEM	Scanning Electron Microscope
SFW	Synthetic Feed Water
SI	Saturation Index
SSA	Specific Surface Area
T(4-CP)P	Porphyrin Colorimetric Method
V_T	Void-space Volume
V_v	Bulk Particle Volume
XPS	X-Ray Photoelectron Spectroscopy
XRD	X-Ray Powder Diffraction
Zn	Zinc
ε	Particle Porosity

LIST OF APPENDICES

Appendix A Media Characterization 69

CHAPTER 1 INTRODUCTION

1.1 Background

Manganese (Mn) is one of the most abundant metals in Earth's crust, and exists in 11 oxidative states, the most environmentally and biologically important of which are Mn^{2+}, Mn^{3+} and Mn^{4+} ((ATSDR), 2012). In water, Mn speciation is controlled by pH and dissolved oxygen (DO), or oxidation/reduction potential (ORP), as well as by its tendency to form a large variety of complexes depending on the available anions ((ATSDR), 2012; EPA, 2004; Stokes, 1988). Surface and ground water (GW) sources of manganese can be natural (from rock and soil weathering) and anthropogenic (from industrial discharges, mining activities and landfill leaching). In GW, detection rates vary in relation to rainfall chemistry, the type of aquifer materials, differences in GW residence times, and redox conditions in the aquifer. In general, anaerobic conditions are dominant in groundwater, which can cause elevated levels of dissolved manganese (Ayotte, Gronberg, & Apodaca, 2011; Stumm & Morgan, 1996). The divalent form Mn^{2+} therefore predominates in most groundwater at pH 4–7, but more highly oxidized forms may occur at higher pH values or result from microbial oxidation ((ATSDR), 2012).

Regulation of Mn concentrations in drinking water has been a recent topic of concern. While it is considered a micro-nutrient essential to the proper functioning of many cellular enzymes, adverse health effects can be caused by an overexposure to Mn. In particular, there is increased evidence of the neurotoxicity of the element (Bouchard et al., 2011; Dion et al., 2018; Oulhote et al., 2014). Although Mn intake from drinking water is normally substantially lower than intake from food, Mn is possibly more bioavailable and metabolized differently when ingested in water (Bouchard et al., 2011; Ljung & Vahter, 2007; Wasserman et al., 2006). Canadian data typically reports values under 100 μg/L of Mn in tap water, however there are cases where levels may reach thousands of micrograms per liter (Canada, 2019). Drinking mineral water regularly therefore has the potential to add significantly to manganese intake. In addition, aesthetic and operational issues caused by high Mn content make the efficient removal of the metal from drinking water a common concern. At concentrations exceeding 20 μg/L, the presence of manganese has led to consumer complaints

about water discoloration and staining of fixtures and laundry (Sly, Hodgkinson, & Arunpairojana, 1990). Based on the above information and the GW conditions in Canada, Health Canada has updated the maximum acceptable concentration (MAC) of Mn in drinking water to 120 µg/L and the aesthetic objective (AO) to 20 µg/L (Canada, 2019). The MAC aims to protect infants from neurological effects, while the AO should reduce consumer complaints regarding discolored water and staining. Both levels can be measured by available analytical methods and are achievable by existing municipal and residential treatment technologies (Canada, 2019).

Residential scale treatments of Mn in GW commonly include catalytic filtration or cation exchange (IX) technologies coupled with point of use reverse osmosis. This Master's work investigates the operational capacity of a calcite ($CaCO_3$) contactor as a polishing step following an alternative Mn removal process using a non-selective hollow fiber nanofiltration (HFNF) membrane (Haddad, Ohkame, Bérubé, & Barbeau, 2018). Such a contactor was previously found capable of correcting the hardness level of a soft influent water comparable to what might be produced in the HFNF process, while removing different Mn concentrations to below 20 µg/L (Pourahmad, Haddad, Claveau-Mallet, & Barbeau, 2019). Pourahmad and co-workers also examined the long-term performance of the calcite contactor in regards to the impact of Mn loading on calcite dissolution and found that a decline in hardness was eventually observed during long term operation with a feed containing high levels of dissolved Mn (Pourahmad et al., 2019). This Master's work investigates the application of a mixed calcite/magnesium oxide contactor with the aim of understanding the contribution of magnesium oxide (MgO) in the remineralization and Mn removal process. We hypothesized that the mixed filter improves Mn retention and hardness release in comparison to a filter bed only composed of calcite.

1.1 Structure of thesis

This thesis is divided into six chapters. Chapter 1 presents a general background on the relevance of manganese in a drinking water context as well as the treatment option investigated in this work. Chapter 2 presents a critical literature review of the application MgO in drinking water treatment for remineralization and contaminant removal purposes. This chapter is in the form of a submitted manuscript to ES&T Water. The consequent research objectives, hypotheses and methodology of

this work are presented in Chapter 3. Chapter 4 presents experimental results and is followed by a general discussion in Chapter 5. Finally, Chapter 6 provides the conclusions and recommendations which have emerged from this work.

CHAPTER 2 ARTICLE 1 - APPLICATION OF MAGNESIUM OXIDE MEDIA FOR REMINERALIZATION AND CONTAMINANT REMOVAL IN DRINKING WATER TREATMENT: A REVIEW

This chapter presents the manuscript submitted to ES&T Water on January 25th, 2021. The article further serves as the literature review for this work.

Application of Magnesium Oxide Media for Remineralization and Contaminant Removal in Drinking Water Treatment: A Review

Authorship

Lena Szymoniak [1], Dominique Claveau-Mallet[1], Maryam Haddad[2], Benoit Barbeau [1]*

Authorship Address

1 Department of Civil, Geological and Mining Engineering, Polytechnique Montreal (QC), Canada, H3C 3A7

2 Department of Chemical Engineering, California State University Long Beach (CA) USA 90840

* Corresponding author: lena.szymoniak@polymtl.ca

Keywords

Magnesium Oxide (MgO), Post-treatment, Water conditioning, Mineral dissolution, Contaminant Removal, Process modelling

Abstract

The post-treatment of desalinated waters is an integral step in the production of quality drinking water. Remineralisation is therefore often essential to stabilize the effluent for distribution and to attain mineral levels which fulfill aesthetic and health goals. According to the World Health Organisation, magnesium (Mg^{2+}) is a nutrient essential to human health. This review summarizes the effectiveness of magnesium oxide (MgO) media for soft water remineralization, as well as its potential for contaminant removal (e.g., Mn, Cu, Zn). We present MgO sources, properties, and dissolution mechanisms. Water treatment applications are then reviewed, and the available design

models critically appraised regarding remineralization and contaminant removal processes. Finally, we discuss the use of MgO in combination with calcite.

2.1 Background and objectives

Access to safe drinking water is fundamental to human health and is therefore considered a basic human right (World Health, 2017). The quality of drinking water can vary from place to place, depending on the chemical, physical, biological, and radiological characteristics of the source water from which it is drawn and the treatment process (McGowan, 2000). In order to deliver safe and high-quality drinking water and minimize aesthetic concerns, pH, alkalinity and hardness of drinking water are routinely monitored during the water treatment process; their interdependence also make them of great importance when determining water treatment targets and operational constraints (Health Canada, 2015). Accepted values of these parameters vary from one legislation to another. The World Health Organisation references approximate guidelines for drinking water pH between 6.5-9.5 and alkalinity and hardness around 60-180 mg $CaCO_3$/L (World Health, 2017).

Naturally soft surface waters and soft treated effluents from desalination processes have low pH, alkalinity and hardness levels. These waters require an effective and cost-efficient method of post-treatment before distribution and consumption in order to achieve target parameter values. While these parameters are most often unregulated, soft water is corrosive and can degrade pipe surfaces, leaching metals and causing possible health concerns regarding regulated contaminants such as copper and lead (World Health, 2017). Additionally, corrosive water can have a metallic or acidic taste, as well as leading to complaints about staining (World Health, 2017). The remineralization process, also called water conditioning or stabilization, typically aims to achieve bicarbonate equilibrium as well as to increase pH and alkalinity. Previous studies recommend a number of remineralization options at the municipal level (Shemer, Hasson, & Semiat, 2015):

- The direct dosage of chemicals such as CO_2, NaOH, $Ca(OH)_2$, $NaHCO_3$, Na_2CO_3, $CaCl_2$, $MgCl_2$, $MgSO_4$;
- Ion exchange resins to modify the effluent mineral level;
- Blending of hard water with a soft effluent;
- Mineral dissolution (e.g., calcite);

- or a combination of the abovementioned methods.

Amongst these options, application of a passive mineral dissolution system at the point of entry (POE) is recommended for residential and small-scale water treatment systems (Letterman, Driscoll, Haddad, & Hsu, 1987). Carbonate media, and particularly calcite (i.e. $CaCO_3$) or limestone contactors, are common residential POE treatment methods due to a simple design which does not require continuous chemical addition, while being inexpensive and easily available in the water treatment market (Shemer et al., 2015). Calcite contactors simultaneously increase carbonate alkalinity, calcium hardness and pH (Birnhack, Voutchkov, & Lahav, 2011). Nonetheless, relying solely on calcite dissolution results in the addition of only Ca^{2+} to the treated water whereas there is increasing evidence regarding the importance of Mg^{2+} in drinking water for human health (Monarca, Donato, Zerbini, Calderon, & Craun, 2006; World Health, 2009). Magnesium oxide (MgO or magnesia) can introduce Mg cations to the effluent and accelerate pH correction owing to the rapid dissolution and hydration of the oxide as $Mg(OH)_2$ (Hasson, Semiat, Shemer, Priel, & Nadav, 2013). A number of studies also document the successful application of MgO media for the removal of divalent metals from wastewater and contaminated groundwater (Caraballo, Rötting, & Silva, 2010; Cortina, Lagreca, De Pablo, Cama, & Ayora, 2003; Courcelles, Modaressi-Farahmand-Razavi, Gouvenot, & Esnault-Filet, 2011; Macías et al., 2012; Navarro, Chimenos, Muntaner, & Fernández, 2006; Oustadakis, Agatzini-Leonardou, & Tsakiridis, 2006; Tobias Stefan Rötting, Cama, Ayora, Cortina, & De Pablo, 2006; Schiller, Tallman, & Khalafalla, 1984; Teringo Iii, 1987). The technical and economic advantages of available remineralisation and post-treatment options have previously been reviewed (Shemer et al., 2015; Withers, 2005). The aim of this review is to provide a comprehensive state of the art summary of the effectiveness of MgO media in soft water remineralization for drinking purposes, as well as its potential for contaminant removal (e.g., Mn, Cu, Zn), an area which has in our opinion been overlooked up to now. Our paper is organised as follows. We present MgO sources, properties, and dissolution mechanisms. Water treatment applications are then reviewed, and we critically appraise the models available for the design of remineralization and contaminant removal processes.

2.2 Magnesium oxide sources and properties

Magnesium oxide is a colourless to grayish white inorganic compound that occurs rarely in nature as the pure mineral periclase (Shand, 2006a). When synthesised, the physical and chemical properties of the mineral are primarily determined by the source of the precursor. MgO is often obtained from magnesite ($MgCO_3$), as well as from seawater or other brines that are rich in $MgCl_2$, where lime (CaO) is added to the brine to produce a magnesium hydroxide ($Mg(OH)_2$) precipitate and $CaCl_2$ brine (Ropp, 2013). The magnesium oxide media is then dehydrated by a calcination process, from which a variety of MgO products with different properties and reactivities can be obtained (Birchal, Rocha, & Ciminelli, 2000). Temperature and time of calcination are the main factors affecting media particle surface area and reactivity. Formed at lower temperatures, the media remains more porous and reactive (Fig. 2.1) (Aphane, van der Merwe, & Strydom, 2009; Birchal et al., 2000; Canterford, 1985; Eubank, 1951; Kato, Yamashita, Kobayashi, & Yoshizawa, 1996; B. Liu, Thomas, Ray, & Guerbois, 2007; Mo, Deng, & Tang, 2010).

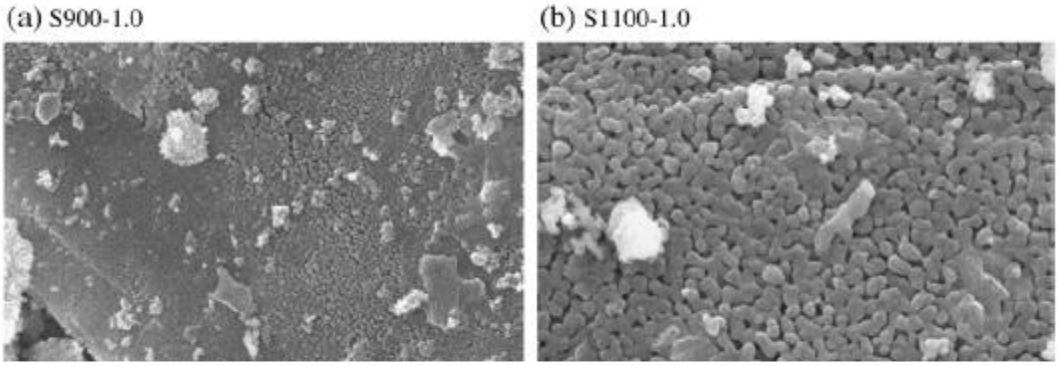

Figure 2.1 Effect of calcination temperature on the morphology of an MgO aggregate. Image (a) shows 1 hour of calcination at 900 °C and (b) at 1100 °C. According to the authors, specific surface area decreased by a factor of 13 for the sample calcined at only 200 °C higher.

This lower temperature product is used in the water treatment industry, due to preferable reactivity and solubility (Shand, 2006a). When calcined at 1500ºC – 2000ºC MgO is used almost exclusively for refractory applications due to its high melting point at 2800ºC (Shand, 2006a).

2.3 Mechanisms in MgO dissolution

For the purposes of reviewing the applications of MgO in the drinking water domain, this section discusses the main phenomena impacting MgO contactors, mainly: dissolution, hydration, precipitation, nucleation, and crystal growth. In water, MgO undergoes an alkaline reaction to form Mg $(OH)_2$, also referred to as magnesium hydroxide, or brucite (Vermilyea, 1969):

$$\mathrm{MgO}_{(s)} + \mathrm{H_2O}_{(l)} \rightarrow \mathrm{Mg(OH)}_{2(s)} \qquad (1)$$

Two main dissolution mechanisms have been proposed in the literature (Birchal, Rocha, Mansur, & Ciminelli, 2002; Kitamura, Onizuka, & Tanaka, 1996; Smithson & Bakhshi, 1969). The first is a shrinking core model applicable at temperatures ranging from 135-200°C, which was modified to incorporate the influence of the hydration layer on the solid reactant (Kitamura et al., 1996; Smithson & Bakhshi, 1969). For temperatures lower than 90°C, which is the case for water treatment, a second mechanism is proposed. This mechanism is based on dissolution and precipitation steps with some variation in the kinetic models and intermediate reactions. A compilation of the three main reaction pathways of the second model is summarised by Rocha and co-workers (Rocha, Mansur, & Ciminelli, 2004):

1) Water simultaneously adsorbs at the surface and diffuses inside porous MgO particles.
2) Oxide dissolution occurs within particles, changing porosity with time:

$$\mathrm{MgO}_{(s)} + \mathrm{H_2O}_{(l)} \rightarrow \mathrm{Mg^{2+}} + 2\mathrm{OH^-} \qquad (2)$$

3) Supersaturation, nucleation, and growth of magnesium hydroxide at the surface of the MgO particle:

$$\mathrm{Mg^{2+}} + 2\mathrm{OH^-} \rightarrow \mathrm{Mg(OH)}_{2(s)} \qquad (3)$$

Hydroxylation and dissolution of the media rapidly increases the concentration of Mg^{2+} and OH^- ions in solution followed by a nucleation process, or induction period (Feitknecht & Braun, 1967; Rocha et al., 2004; Vermilyea, 1969). Once the concentration of Mg^{2+} and OH^- ions in water has reached the saturation level, the precipitation (hydration) step begins (Rocha et al., 2004). Although Glasson suggested in 1963 that the continued dissolution of MgO is practically unimpeded by the hydration layer (Glasson, 1963), others claim that the hydration process would slow down further

oxide dissolution and that the Mg $(OH)_2$ layer becomes rate determining (Birchal et al., 2002; Rocha et al., 2004; Smithson & Bakhshi, 1969; Tang et al., 2014; Vermilyea, 1969). We therefore consider the latter dissolution-precipitation mechanism in this review, as it is more commonly observed in the literature.

Solubility has been cited as low as ~5 to 9 mg/L (~12 to 21 mg $CaCO_3$ eq/L) at 30°C without specifying further conditions (Schiller et al., 1984; Shand, 2006a, 2006b). However, at room temperature and in acid-free desalinated water, solubility has also been measured to be as high as 34 mg/L (~84 mg $CaCO_3$ eq/L) (Hasson et al., 2013). Furthermore, although the oxide solubility is not found in reference texts such as *Aqueous Environmental Geochemistry*, the hydration product Mg $(OH)_2$ is cited at a significantly higher K_{sp} than that of calcite (Table 2.1) (Langmuir, 1997). As it is generally accepted that MgO rapidly reacts to form $Mg(OH)_2$ and that dissolution of the latter is rate determining, this second measurement appears to be more appropriate when compared to the known solubility of calcite (14 mg $CaCO_3$/L).

Table 2.1 Solubility products at 25°C and 1 bar total pressure.

Mineral	**Formula**	**K_{sp} expression**	**-log K_{sp}**
Brucite	$Mg(OH)_2$	$[Mg^{2+}]\,[OH^-]^2$	11.16
Calcite	$CaCO_3$	$[Ca^{2+}]\,[CO_3^{2-}]$	8.48

In 2002, Birchal and co-workers proposed a dissolution-precipitation model for a range of temperatures and were able to validate it at lower temperature (35°C). Their kinetic model incorporated a factor of resistance as a result of the change in the porosity of media over time (Birchal et al., 2002). According to this model, Mg $(OH)_2$ forms and deposits in the pores of the MgO particles, and the buildup of a hydroxide film increases the resistance of the media to further dissolution and hydration. This process is described by a semi-empirical equation which includes the mass balance of $Mg(OH)_2$ produced during hydration (Birchal et al., 2002).

$$C_{Mg(OH)_2}(t) = C^0_{MgO} - C^0_{MgO}\exp\left[\frac{b}{a}(1 - e^{at})\right] \qquad (4)$$

Where $C_{Mg(OH)_2}(t)$ is the concentration (mol/m^3) of the hydration product at a given time of reaction t (h), which is a function of the initial media concentration C^0_{MgO} and its dissolution and hydration over time. The model also introduces the parameter *a* as a rate constant (h^{-1}) describing the variation of the porosity with time at a set temperature. Fitting transient experimental porosity data in the following equation obtains *a:*

$$\varepsilon(t) = \frac{\varepsilon^0}{\varepsilon^0 + (1-\varepsilon^0)\exp(-at)} \qquad (5)$$

Where ε^0 and ε (t) are the initial porosity and porosity at a given reaction time, respectively. The temperature dependence is included in parameter *b*:

$$b = \frac{\varepsilon^0 a_v}{1-\varepsilon^0} k_0 \exp\left(-\frac{E}{RT}\right) \qquad (6)$$

Where a_v is the area per volume of the media (m^2/m^3), E is the reaction activation energy, R is the universal gas constant, T is the temperature (°C), and k_0 is the initial reaction constant (m^4/(mol•h). Although the model was not able to predict the behavior of the authors' experimental samples hydrated below 35°C, subsequent work confirmed that it well described experimental data for MgO in pure water at 30-90°C (Rocha et al., 2004; Tang et al., 2014).

The Johnson & Mehl, Avrami and Kolmogorov (JMAK) model is a common approach used to describe the nucleation and growth in the hydration process. This model assumes nucleation distributed randomly throughout the total volume of the reaction system (Avrami, 1939; Johnson & Mehl, 1939; Kolmogorov, 1937). However, hydration products have been found to form on the boundary of MgO grains (Jägle & Mittemeijer, 2011; Mo et al., 2010). A related boundary nucleation and growth (BNG) model incorporates such preferential nucleation (Cahn, 1956). Experimental results of MgO hydration have confirmed a better fit with an adapted form of the BNG over the JMAK model, especially at lower temperatures (20°C–50°C) (J. P. Liu, Wang, Tian, & Zhang, 2012; Thomas, 2007; Thomas, Musso, & Prestini, 2014). The BNG model can be written as:

$$C_{Mg(OH)_2}(t) = 1 - \exp\left[-2O_V^B \int_0^{Gt}\left(1 - \exp(-Y^e)\right)dy\right] \qquad (7)$$

Where $Y^e = \frac{\pi I_b}{3} G^2 t^3 \left[1 - \frac{3y^2}{G^2t^2} + \frac{2y^3}{G^3t^3}\right]$ (if $t > y/G$) and $Y^e = 0$ (if $t < y/G$)

G is the linear rate of growth of a product region in any direction, O_V^B is the boundary area per unit volume on which nucleation can occur and I_b is the nucleation rate per unit area of the fresh MgO surface. The kinetics of the boundary nucleation process can be further described by two rate constants with units of inverse time (Thomas, 2007):

$$k_B = (I_B O_V^B)^{\frac{1}{4}} G^{\frac{3}{4}};\ k_G = O_V^B G \quad (8)$$

The rate constant k_B describes the rate at which the particle surface is covered with the hydration product, whereas k_G describes the rate at which the hydration product fills pore spaces between the particles. If $k_B \gg k_G$, the boundary regions will be densely populated with nuclei and the media will hydrate completely early in the overall process (Thomas, 2007). This scenario projects a thickening of the Mg $(OH)_2$ layer centered on the original MgO surface and predicts the hydration rate to decrease exponentially with time. However, if $k_B \ll k_G$ holds, the internal boundaries are expected to be only sparsely populated with nuclei. Media hydration would, therefore, occur essentially at the same rate in the entire system as described by the standard Avrami equation (Thomas, 2007).

From the literature, it is apparent that the models proposed by both Birchal and Thomas were able to adequately describe the dissolution and hydration of MgO powders at lower temperature. While the model presented by Birchal offers a numerically simpler representation of the hydration effects, only the modified BNG model has been verified at temperatures as low as 20°C, which is the most representive of a water treatment context. Neither, however, have been applied to granular MgO. In a design context, it would therefore be crucial to verify that these theoretical models can simulate the dissolution and hydration behavior of a granular MgO column.

2.4 Parameters affecting MgO dissolution in water treatment

The overall rate of MgO dissolution and hydration is expected to be controlled by the diffusion of dissolved reactants and products or by surface reaction, depending on the system conditions (Fruhwirth, Herzog, Hollerer, & Rachetti, 1985; Jones, Segall, Smart, Turner, & Craig, 1981; Jordan, Higgins, & Eggleston, 1999; Segall, Smart, & Turner, 1978; Vermilyea, 1969; Wogelius, Refson, Fraser, Grime, & Goff, 1995). The application of MgO in water treatment is therefore influenced by several factors, which we examine below.

2.4.1 Media Impurities

The rate of media dissolution is determined by the physical and chemical characteristics of the particle, including the type and the amount of impurities in the mineral composition (Eisenlohr, Meteva, Gabrovšek, & Dreybrodt, 1999). In the presence of impurities, media dissolution may initially be controlled by more soluble fractions (Cortina et al., 2003). Several researchers suggested that CaO present in small quantities in caustic magnesia can initially control dissolution and solution pH response until exhausted (Cortina et al., 2003; Tobias Stefan Rötting et al., 2006). In practice, we might expect this to result in a pH spike at the beginning of column operation before effluent pH stabilises.

2.4.2 Particle Size and Shape

Particle size influences media contact surface area and consequently, the reaction surface between media and water. As particle size increases, the surface area in contact with water decreases, and extended contact times are required to attain the same degree of dissolution and hydration (Tobias S. Rötting, Ayora, & Carrera, 2008). In a kinetic study of MgO dissolution, single-crystal surfaces exposed to aqueous environments for several days showed no evidence of hydration, while highly defective surfaces and powders with higher surface areas converted readily to brucite (Mejias, Berry, Refson, & Fraser, 1999). The reactivity of MgO therefore appears to be directly linked to its size, shape and specific surface area, which determine the available adsorption sites (Kameda, Yamamoto, Kumagai, & Yoshioka, 2020). Aside from dissolution and reactivity effects, particle size plays an important role when determining a filter porosity that ensures sufficient permeability of media in an engineering application (Navarro et al., 2006). Commercially, the effective particle size (D_{10}) of granular MgO sold for NSF approved drinking water treatment ranges from approximately 1.2-3.5 mm.

2.4.3 Internal Particle Porosity

MgO media material consists of a solid matrix with interconnected voids, referred to from here on out as particle porosity. Particle porosity can be generally described as the ratio of void-space volume (V_v) to bulk particle volume (V_T) (Stumm & Morgan, 1996):

$$\varepsilon = \frac{V_V}{V_T} \qquad (9)$$

This should not be interpreted as the porosity of the filter bed, which considers the volume of voids between particles and contributes to the permeability of the filter (Nield & Bejan, 2017). Particle porosity is known to be positively correlated to specific surface area (SSA), which is directly proportional to the hydration degree of MgO particles (Jin & Al-Tabbaa, 2014; Smithson & Bakhshi, 1969). As a result, MgO reactivity decreases remarkably with a lower SSA (Jin & Al-Tabbaa, 2014; Mo et al., 2010). In 2014, Jin & Al-Tabbaa observed a hydration limit due to the incomplete hydration of the most interior area of magnesia particles (Jin & Al-Tabbaa, 2014). They found that the hydration degree increases linearly with the increase of specific surface area (SSA) before this limit is reached (Jin & Al-Tabbaa, 2014). Alteration of initial particle porosity caused by the precipitation of $Mg(OH)_2$ has also been reported in the literature (Rocha et al., 2004; Tang et al., 2014). As the reaction progresses, both the surface and pores of magnesia particles are progressively covered by a hydroxide film, changing the porosity of the media (Rocha et al., 2004). Accordingly, the diffusion of water is hindered inside particles, reducing the overall reaction rate through diffusive control (Rocha et al., 2004). In practice, this phenomenon implies that pH and alkalinity are not expected to be stable over the operation cycle of a contactor, with higher values predicted with fresh media.

2.4.4 Feed water composition

2.4.4.1 Acidity (pH)

Kinetic theories concerning the dissolution of ionic oxides predict that their dissolution rate exhibits an inverse exponential dependence on solution pH (Blesa, 1994; Gorichev & Kipriyanov, 1984; Segall et al., 1978; Vermilyea, 1969). In 1969 Vermilyea proposed a control of MgO dissolution by proton attack at low pH and proton diffusion at higher pH (Vermilyea, 1969). Fruhwirth and co-workers studied rate-controlling processes by conductivity and scanning electron microscopy measurements during and after hydration experiments. They found that the hydration rate of MgO is controlled by the dissolution rate, with the overall reaction being limited by H^+ and OH^- diffusion (Fruhwirth et al., 1985).

2.4.4.2 MgO saturation index

The saturation state of the solution in contact with MgO media and hydrated Mg $(OH)_2$ surfaces controls for a large part the extent of media dissolution. In general, the saturation index (SI) of a mineral phase can be calculated using the ion activity product (IAP) and solubility constant K (Stumm & Morgan, 1996):

$$\mathrm{SI} = \log(\mathrm{IAP}/\mathrm{K}) \qquad (10)$$

Saturation is influenced by pH and temperature, and more specifically the difference between the solution pH and the saturation pH (pH_{eq}) which can be calculated for a system at a given temperature (Stumm, 1997). When SI <0 or the solution pH is less than calculated equilibrium pH, the mineral phase is expected to dissolve, as the solution is under saturated. Precipitation occurs when SI >0, or the when the solution pH exceeds pH_{eq} and the system is supersaturated with respect to the mineral phase (Stumm & Morgan, 1996). Furthermore, SI dictates if precipitation will be homogeneous (high SI) or heterogeneous (low SI). These equilibrium principles will govern the extent of dissolution of MgO in water treatment, with influent pH and temperature acting as important factors in determining the remineralisation capacity of the media.

2.4.4.3 Temperature

The temperature dependence of the MgO hydration reaction rate constant is consistent with an Arrhenius-type formulation (Bratton & Brindley, 1965; Fruhwirth et al., 1985; Layden & Brindley, 1963). The solubility of the hydration product $Mg(OH)_2$ has been found to decrease as the temperature of the system increases (Rocha et al., 2004; Vermilyea, 1969). Consequently, MgO media experiences accelerated hydration and reduced solubility with increasing temperature (Amaral, Oliveira, Salomao, Frollini, & Pandolfelli, 2010; Fedorockova & Raschman, 2008; Glasson, 1963; Tang et al., 2014; Thomas et al., 2014). It should be noted that a high supersaturation and nucleation rate can be reached rapidly within a few minutes even at a lower temperature of 35°C (Rocha et al., 2004). This is of particular interest because it suggests that at low temperature, $Mg(OH)_2$ precipitates as small particles, which form a very porous agglomerate on the media surface (Rocha et al., 2004). Moreover, the morphology and distribution of the Mg

$(OH)_2$ hydration product appears to change with temperature, which in turn impacts the reaction kinetics (Thomas et al., 2014).

2.4.4.4 Aqueous CO_2 content

The maximum magnesium ion concentration that can be achieved by magnesia dissolution in acid-free soft water is limited by the low equilibrium solubility 34 mg/L (84 mg $CaCO_3$/L) (Shemer et al., 2015). The extent and rate of MgO dissolution can be enhanced by acidifying the inlet solution with CO_2. It has been found that in water, MgO and $Mg(OH)_2$ react at the same rate with aqueous CO_2 (Evans & Clair, 1949). These similar rates could be explained by the fact that media dissolution is inhibited by the $Mg(OH)_2$ hydration layer present on the surface of MgO which further confirms the rapid formation of a rate controlling hydration film (Smithson & Bakhshi, 1969). In addition to shifting the system solubility equilibrium, the presence of available dissolved CO_2 can promote the precipitation of magnesite ($MgCO_3$) or partially recrystallize the hydration layer to hydromagnesite rather than solely hydrating MgO as $Mg(OH)_2$ in pure water (Brown et al., 1999). Figure 2.2 compares the theoretical solubility of calcite or MgO in pure water at 25°C. We assume the hydration of MgO such that dissolution is rate limited by the hydration product $Mg(OH)_2$ and use the K_{sp} values provided in Table 2.1. Solid lines are simulated in a closed system, where the influent is not equilibrated with CO_2 (g) before entering the batch simulation. The respective $CaCO_3$ and MgO hardness release can be seen increasing significantly with influent alkalinity in Fig. 2.2A, which indicates the importance of dissolved CO_2 on media solubility. The simulated variation in media solubility and consequent hardness response for influents exposed only to atmospheric CO_2 (410 ppm) appears to be minimal (2 mg $CaCO_3$/L) in comparison. It should be noted that alkalinity varies significantly across the pH range described by this simulation. For example, the addition of 25 $CaCO_3$/L alkalinity as 0.0006 M $NaHCO_3$ results in alkalinities ranging from 10 to 30 along the same closed system curve with increasing pH. Fig. 2.2B further suggests that the pH correction and remineralization capacity of $CaCO_3$ is more sensitive to the presence of dissolved CO_2 than that of MgO. In the closed system simulations, we see that increasing influent alkalinity increases the effluent pH range as well as the range of effluent hardness levels. While MgO also experiences improved hardness release in response to increasing concentrations of $CO_{2\,(aq)}$, its pH response remains more stable. In pure water and a closed system,

the simulation data appears as a cluster of points rather than a curve. This confirms that without the presence of $CO_{2\,(aq)}$, both media experience a very narrow dissolution range and consequently produce an effluent with more controlled pH correction. In a treatment context, $CO_{2\,(aq)}$ therefore remains of great importance not only in optimising the remineralization capacity of the media, but in understanding the sensitivity of effluent water quality to variation in influent $CO_{2\,(aq)}$.

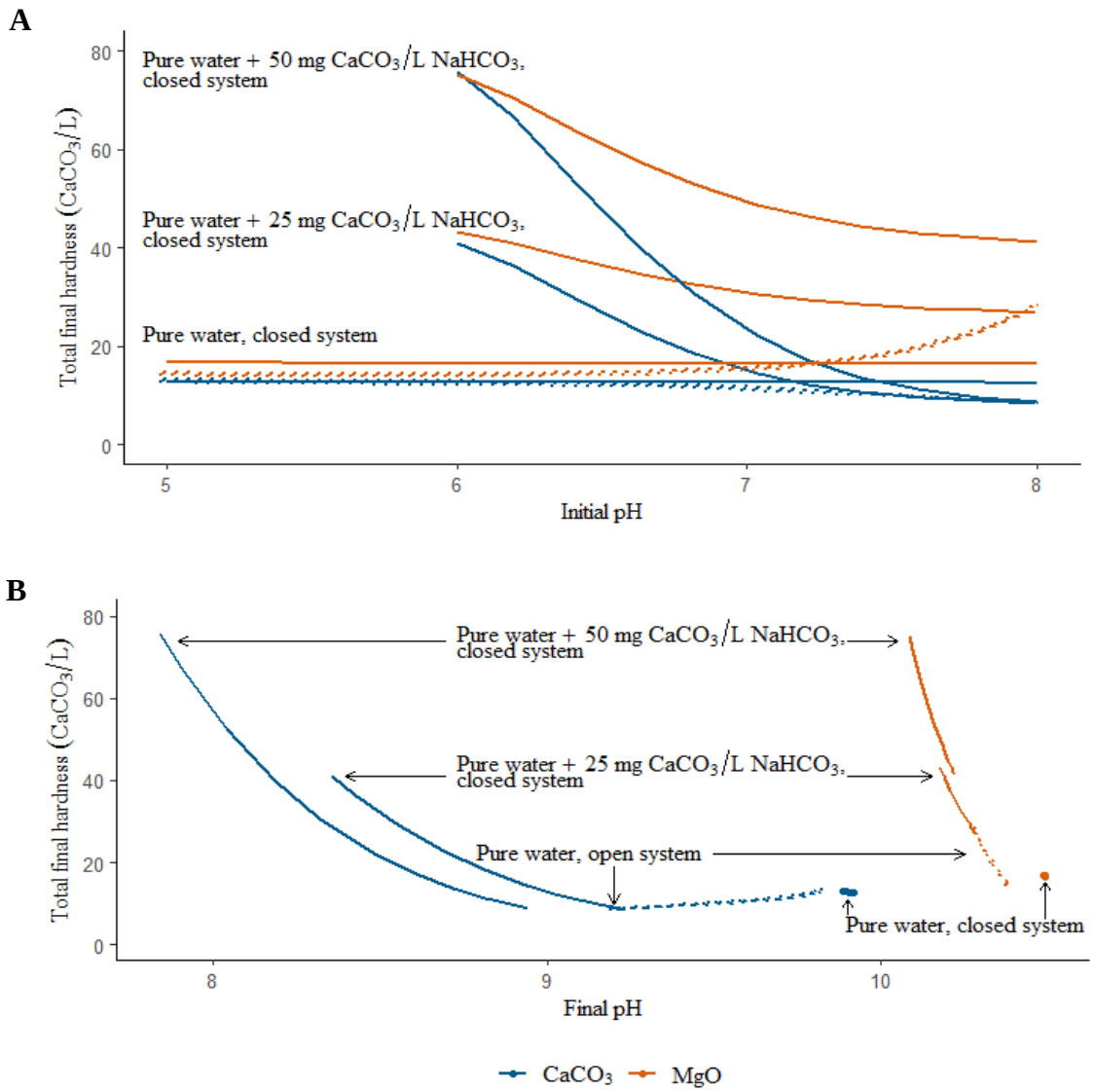

Figure 2.2 A) Theoretical solubility curves for pure $CaCO_3$ or MgO, in open (dotted) and closed (solid) systems. Before entering the batch simulation, the influent has zero Ca^{2+} or Mg^{2+} hardness and is prepared at varying pH by the addition of HCl or NaOH. B) Corresponding effluent pH following the dissolution of each media.

2.4.4.5 Presence of anions

The presence of anions other than OH^- can form a hydration barrier by competing with OH^- for the positively charged $MgOH^+$ surface during the dissolution process (Amaral et al., 2010). For example, the authors reported a delay in the MgO hydration reaction when $CaCl_2$ was added to the solution (Amaral et al., 2010). However, if the anion competition results from the dissolution of a magnesium salt (i.e., $MgCl_2$), the common ion effect increases Mg^{2+} concentration. Rather than delaying hydration due to the formation of a protective anion layer, magnesium supersaturation is accelerated and the precipitation of $Mg(OH)_2$ was found to be more effective (Amaral et al., 2010). Vermilyea also noted that certain dissolution accelerators such as phosphate can form protonated ions that react directly with the surface hydroxyl, and, subsequently, increase brucite dissolution (Vermilyea, 1969). However, in the context of soft water treatment, we do not expect the concentration of influent anions to be significant enough to impact the dissolution of MgO media.

2.4.4.6 Presence of dissolved metals

Dissolved metals can form local, unreactive MeO(OH) networks on oxide and carbonate surfaces (Stumm, 1997). Among divalent metals (Me^{2+}), Pb and Ca cations promoted $Mg(OH)_2$ dissolution and Co and Ni inhibited dissolution rates at room temperature and slightly acidic pH (4.9) (Pokrovsky, Schott, & Castillo, 2005). In a water treatment context, the interaction of dissolved metals with a mineral surface becomes especially interesting if it leads to the retention of the metal. Using calcite for the remineralization and simultaneous removal of manganese from a synthetic feedwater, Pourahmad and co-workers found that the media was progressively loaded with a stable MnO_x film (Pourahmad et al., 2019). The authors proposed that upon initial removal as $MnCO_3$ through an ion exchange sorption reaction, the metal carbonate slowly recrystallizes as MnO_2. The authors also observed improved metal removal due to the autocatalytic nature of the adsorption and oxidation of remaining dissolved manganese by the oxide film. MgO is also known to be an effective media in the treatment of dissolved metals, as discussed in further detail below.

2.4.4.6.1 Precipitation

The most common method for removing metals from solution is by adjusting the pH in order to precipitate the metal as its hydroxide (Shand, 2006b):

$$Me^{n+} + nOH^{-} \rightarrow Me(OH)_n \quad (12)$$

Although the dissolution of carbonates allows for the removal of trivalent metals through precipitation, efficient divalent metal removal (i.e. Zn, Mn, Cu, Pb, Ni, Co and Cd) requires a higher pH range (9-10) produced by the dissolution of MgO (Cortina et al., 2003). The solubility and surface charge of MgO also favors the formation of compact precipitates, as the precipitation reaction occurs at the positively charged hydroxylated surface; whereas the formation of a hydroxide suspension would mainly take place in the presence of more soluble bases (Schiller et al., 1984).

2.4.4.6.2 Sorption

The difference between MgO metal removal by sorption or precipitation is not thoroughly addressed in the literature. Studies on $Me(OH)_x$-H_2O interactions suggest that hydroxide particles can remove metals within a periphery of localised high pH close to the particle surface, even in cases where the bulk solution pH does not precipitate metals from solution (Frost et al., 1990; Teringo Iii, 1987). While some researchers suggested that the dissolution of MgO promotes the oxidation of metal hydroxides into negatively charged metal oxides, which sorb metal cations remaining in solution (Balintova & Petrilakova, 2011; Cao, Qu, Wei, Liu, & Song, 2012; Choi, Woo, Jang, Cannon, & Snyder, 2014; Hövelmann, Putnis, & Benning, 2018; Navarro et al., 2006; Tobias Stefan Rötting et al., 2006). As a combined mechanism, metal removal could therefore be considered a sorption-coprecipitation process (Navarro et al., 2006).

2.4.4.6.3 Cation exchange

Cao and co-workers suggested a direct cation exchange between the magnesium cation and the divalent contaminant ion rather than removal by sorption to the oxidized metal hydroxide. They justify this mechanism by the quantitative measurement of the molar amount of Mg^{2+} released and the amount of Pb^{2+} or Cd^{2+} adsorbed in batch experiments, finding a liner relationship (Cao et al., 2012). While we were not able to find any other work investigation the metal removal by cation exchange for MgO, previous research has found that calcite effectively removes Me^{2+} from solution by such a mechanism (Pourahmad et al., 2019).

2.5 Comparison to calcite dissolution

There are several theoretical models for calcite dissolution, most importantly including those of Plummer, Parkhurst and Wigley (PWP), Yamauchi, and Letterman (Letterman et al., 1987; Plummer, Wigley, & Parkhurst, 1978; Yamauchi, Tanaka, Hattori, Kondo, & Ukawa, 1987) . In the Yamauchi and PWP models, the phenomenon of diffusional mass transport is neglected in favor of surface reactions, while Letterman assigns mass transfer as the key controlling mechanism in predicting calcite dissolution. Modifications have been proposed by several researchers to better simulate contactor experimental data (Buhmann & Dreybrodt, 1985; Chou, Garrels, & Wollast, 1989; Dreybrodt, Lauckner, Zaihua, Svensson, & Buhmann, 1996; Svensson & Dreybrodt, 1992).

Although reviewing the $CaCO_3$ system would be beyond the scope of this work, more in-depth reviews can be found elsewhere (Hasson & Bendrihem, 2006; Morse, Arvidson, & Lüttge, 2007; Plummer, Parkhurst, & Wigley, 1979). As $CaCO_3$ is a prevalent media used within the treatment context reviewed here, it is worth mentioning that the parameters discussed in section 2.2 exhibit the same tendency to stimulate or hinder the dissolution of both MgO and $CaCO_3$ minerals. This is important for the engineering application, as it allows for the design to optimise the dissolution of both media without hindering the other. However, while the changes in these parameters produce the same general effect on the dissolution of MgO and $CaCO_3$, the media response remains different. Notably, both media experience increased dissolution rates at lower pH (Fig. 2.2), whereas their mineral phases stabilize at different equilibrium pH (Langmuir, 1997). This is especially important to consider in the water treatment context as pH can significantly impact metal removal. In addition, a mixed $CaCO_3$/MgO contactor will be unable to attain equilibrium concentrations for both minerals, which will impact respective Ca^{2+} and Mg^{2+} remineralization (Ginocchio, 1985). Both aspects are discussed in detail in the following section on water treatment applications.

2.6 Water treatment applications

In drinking water systems, remineralization is often implemented as a polishing step at the end of the treatment chain. This is the case for naturally soft ground or surface waters and desalinated waters. For treated water, the effluent may require remineralization following non-selective

processes such as reverse-osmosis (RO) and other membrane applications such as nano-filtration, which deplete water hardness and alkalinity. Importantly, most conventional post-treatment technologies do not enrich water with Mg^{2+}, especially at the smaller, domestic scale (Shemer et al., 2015). Mineral sources of Mg^{2+} in the water treatment industry include dolomite ($CaMg(CO_3)_2$) and MgO media. Although not explicitly recommended in the literature, it appears that it may be advantageous to implement a $CaCO_3$/MgO blend, rather than using $CaMg(CO_3)_2$. For example, Luptáková and co-workers found that magnesium content dominated in treated water when using half-calcined dolomite and suggested the use of dolomite with higher Ca content for more balanced effluent target values (Luptáková & Derco, 2015). However, dolomite is known to be naturally more heterogenous than limestone (Machel, 2005). This requires a dolomite-based re-mineralization system to exhibit a greater design-flexibility compared to a conventional calcite contactor (Shemer et al., 2015). Most literature reports based on laboratory batch tests also indicate that dolomite dissolution is much slower compared to that of calcite while MgO is known to be significantly more soluble than $CaCO_3$ (Chou et al., 1989; Z. Liu, Yuan, & Dreybrodt, 2005; Morse & Arvidson, 2002). In addition to preferable reaction kinetics, MgO mixed with $CaCO_3$ rather than the use of solely dolomitic media could offer a greater adaptability of the Ca/Mg remineralization ratio as well as improved control of pH adjustment required for divalent metal removal.

In drinking water treatment, it is recommended to use chemicals that are NSF International (NSF) or American National Standards Institute (ANSI) certified. *NSF/ANSI Standard – 60* for *Drinking Water Treatment Chemicals* applies to process media accepted in water treatment and distribution systems. In North America, Martin Marietta Magnesia is the currently the only *NSF/ANSI Standard 60* supplier of MgO media products for pH adjustment or precipitation processes.

2.6.1 Main applications

2.6.1.1 pH & alkalinity correction

Waters with low pH and alkalinity are considered soft and corrosive, while a high pH level is often associated with a higher mineral content in the form of alkalinity and hardness. MgO dissolves readily in aqueous environments, and the hydration product $Mg(OH)_2$ controls residual effluent pH and alkalinity. The $Mg(OH)_2$ film releases OH^- slowly over time, due to its low aqueous solubility

(Pishtshev, Karazhanov, & Klopov, 2014; Tobias Stefan Rötting et al., 2006). Following an initial rapid pH increase with MgO dissolution, the stabilised effluent pH is therefore constrained by Mg $(OH)_2$ dissolution, providing a long-term source of OH^- alkalinity at a pH range of 9-11 (Caraballo et al., 2010; Hiortdahl & Borden, 2014; Kameda, Takeuchi, & Yoshioka, 2009; Navarro et al., 2006). Compared to operating a conventional limestone contactor, authors have found that MgO media used in column experiments of comparable dimensions was able to remove twice the acidity (in $CaCO_3$ equivalents) (Caraballo, Rötting, Macías, Nieto, & Ayora, 2009; Tobias Stefan Rötting et al., 2006). Figure 2.3 summarises the main reaction mechanisms that occur in the treatment application of MgO and calcite, respectively. For drinking water applications, the application of MgO on its own risks producing an 'over-corrected' water. The media is therefore of great interest as an addition to the standard calcite contactor, moderating the pH correction as well as producing a remineralized water with both Ca^{2+} and Mg^{2+} hardness.

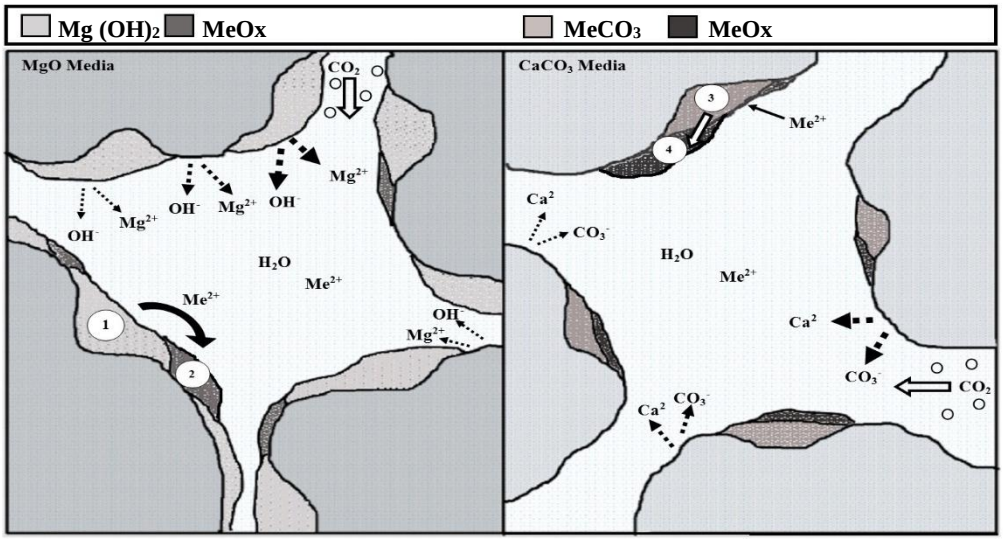

Figure 2.3 Comparative summary of MgO and $CaCO_3$ remineralization in soft water containing dissolved divalent metals. The thickness of the dashed arrows indicates relative reaction kinetics, and the presence of CO_2 increases the dissolution of the two media and the MgO hydration product, $Mg(OH)_2$. The main reactions in each system are as follows: 1) rapid hydration of MgO into $Mg(OH)_2$, and 2) removal of Me^{2+} by oxidation and sorption-coprecipitation process or possible cation exchange. In a $CaCO_3$ system the Me^{2+} is removed by 3) ionic exchange, followed by 4) the slow recrystallization of $MeCO_3$ to MeO_2.

2.6.1.2 Magnesium hardness

In the last decade, guideline recommendations have been adapted to include the importance of Mg^{2+} alongside Ca^{2+} in the potential health benefits of mineral drinking water (World Health, 2009). Since then, several workers have adapted treatment chains to include magnesium addition to the water conditioning process. However, this includes only a few which aim to introduce magnesium hardness through the application of MgO media (Hasson et al., 2013; Pourahmad et al., 2019; Schwartz, Shemer, Hasson, & Semiat, 2015). Both Hasson and Schwartz focus on Mg^{2+} remineralization, the latter improving the dissolution process with either CO_2 or H_2SO_4 injections at the inlet of pure MgO columns (Hasson et al., 2013; Schwartz et al., 2015). Working at a scale more appropriate for domestic application, Pourahmad and co-workers successfully adapted a pure calcite contactor to improve long term remineralization of drinking water by introducing a fraction of MgO into the column (Pourahmad et al., 2019). It appears that despite being a media well known to the industry, the investigation of MgO remineralization for drinking water purposes has been somewhat overlooked in the research field.

2.6.1.3 Metal removal

While there is relatively little literature addressing the use of MgO for metal removal in drinking water, it is well established in the field of wastewater and contaminated groundwater treatment. MgO powder is used as an alkaline material to facilitate oxidative precipitation, followed by coagulation and flocculation (Huang & Liu, 1995) in waste water treatment applications. Cortina and co-workers showed that MgO meets the conditions for application as a passive *in situ* reactive barrier (PRB) for groundwater treatment, notably due to satisfactory reactivity, permeability, and durability (Cortina et al., 2003). Conventional active treatments typically rely on the continual addition of energy and/or chemical reagents to remove metals, which is costly (Younger, Banwart, & Hedin, 2002). While passive treatments are less precise and require careful design and characterization of the influent to be treated, they generally require lower capital, maintenance, and operating costs than an active system (Skousen et al., 2017). The same arguments that support the use of MgO as a geochemical passive treatment option in the wastewater industry make it appealing for use in smaller systems in the drinking water industry. In these systems, the media reduces metal concentrations by precipitation and sorption mechanisms while requiring minimal maintenance.

Efficient removal of divalent metals has been incorporated into multi and single step passive treatment systems using reactive tanks, columns and permeable reactive barriers (Caraballo et al., 2009; Caraballo et al., 2010; Courcelles et al., 2011; de Repentigny, Courcelles, & Zagury, 2018; De Repentigny, Zagury, & Courcelles, 2019; Macías et al., 2012; Navarro et al., 2006; Oustadakis et al., 2006; Tobias Stefan Rötting et al., 2006; Schiller et al., 1984; Teringo Iii, 1987). In numerous of these studies, the long-term operation of an MgO column eventually suffered from reduced performance due to media coating and decreased permeability. It has also been noted that coarser grained (2-4 mm) MgO columns were much less reactive and exhibited a reduced rate of pH adjustment and dissolved metal removal (Tobias S. Rötting et al., 2008). Constraining MgO reactivity can be undesirable when working with the high contaminant loads common to wastewater treatment. However, in a drinking water context concentrations are expected to be lower and increasing the media particle size could therefore be of interest in order to constrain the treated water pH.

2.6.2 Scale formation

In the water treatment industry, scaling can become an issue both during the treatment operation and during the distribution of the treated effluent. Scaling occurs when the pH, temperature and mineral content conditions are such that saturation thresholds are exceeded, and minerals precipitate, as discussed in section 2.4. The deposition of $Mg(OH)_2$ can be promoted by an increase in temperature or pH, or a decline in dissolved CO_2 (Chilingar, Mourhatch, & Al-Qahtani, 2008). It is therefore critical to monitor these parameters in order to avoid unwanted scaling. Distribution networks that include water heaters are of specific interest, as treated water is subjected to a significant rise in temperature. For magnesium, historical data obtained from studies where magnesium hydroxide precipitation in hot-water tanks and lines was problematic suggests that an effluent at 24°C should have a pH of less than 9.0 and a magnesium hardness of less than 40 mg $CaCO_3$/L in order to avoid scaling in water heaters (Larson, Lane, & Neff, 1959). In practice, the calculation of saturation indices is used to predict the tendency and extent of precipitation. Furthermore, a treated water is unlikely to contain only magnesium hardness. Predictive tools such as proposed by Bahadori (2010) offer an approach to assess operational issues and includes the magnesium contribution to estimate scaling (Bahadori, 2010).

2.6.3 Issues with media coating

As mentioned previously, several authors note a performance decrease in MgO water treatment systems due to media coating leading to reduced system permeability. While initial studies performed by Navarro and co-workers did not find targeted metal removal to be affected by the presence of other metals, other workers later found that aluminum (Al) and iron (Fe) should preferably be removed prior to MgO water treatment in order to prevent prematurely clogging the column (Caraballo et al., 2010; Navarro et al., 2006; Tobias Stefan Rötting et al., 2006). These authors also noted a decrease in column efficiency due to media coating and passivation when only a small portion of the reagent had been consumed (Caraballo et al., 2009; Tobias Stefan Rötting et al., 2006). Results also showed that grain size selection is an important factor influencing the extent of dissolution, and that the proportion of MgO when mixing with another media needs to be adapted to extend operation lengths. Notably, the above column experiments investigated the treatment of acid mine drainage (AMD) with high inlet contaminant concentrations of up to 300 mg/L of aluminum and 100 mg/L iron (Caraballo et al., 2009; Tobias Stefan Rötting et al., 2006). The contaminant concentrations in these studies significantly exceed concentrations expected in drinking water sources.

The operational lifespan of a treatment relying on MgO dissolution has been improved by mixing the alkaline material with a larger inert matrix such as quartz sand or wood chips. This allows for the reduction of MgO grain size, increasing reactivity and specific surface in order to retard passivation while the system permeability remains high (Cortina et al., 2003; Tobias S. Rötting et al., 2008). The use of fine-grained media also allows for more complete dissolution before the growing layer of precipitates passivates the particle. Over a year, it was found that despite a substantial decrease of hydraulic conductivity, finer-grained column experiments treating high zinc and manganese concentrations did not clog at any time (Tobias S. Rötting et al., 2008). In drinking water treatment, interference from high metal concentrations would not be expected once at the point of remineralization. However, it remains interesting to note that within the range of maximum acceptable concentrations (MAC) allowed for Al (2.9 mg/L) and Mn (0.12 mg/L) (Health Canada, 2015), an MgO column may be able to further reduce regulated contaminant levels.

2.6.4 Process design and process control by modelling

The process design of an MgO based drinking water treatment depends on the scale of operation and requires (as most treatments do) a design based on specific treatment targets and influent water characteristics. Modelling can be useful to verify design robustness and to predict the operational capacity and lifespan of a given scenario.

2.6.4.1 Design objectives

To the best of our knowledge, there is currently no commercial software available to guide the design of a MgO or blended $CaCO_3$/MgO contactor for drinking water applications. The models presented in this section concern other types of water treatment applications and are restricted to fixed bed, up flow granular column experiments, as such configuration is the most common option for MgO application in drinking water treatment. Furthermore, all models investigate the dissolution of $Mg(OH)_2$, since the MgO media is considered to hydrate almost instantaneously. There are four main phenomena of interest when simulating column treatment:

1) Dissolution;
2) Particle evolution and passivation;
3) Contaminant removal; and
4) Permeability loss.

Table 2 summarizes the main approaches to modeling MgO column treatment, according to the phenomena listed above. While several workers have successfully modeled this system, their focus varies depending on the treatment objective and never encompass all four phenomena. For example, a reactive transport model was able to simulate measured depth profiles and was used to extrapolate the lifespan of an MgO column applied for divalent metal removal (Macías et al., 2012; Tobias S. Rötting et al., 2008). Other authors were also able to reproduce laboratory results for metal retention through the geochemical modeling of saturation indices and comparison with confirmed mineral phases along the depth profile of MgO columns (Caraballo et al., 2009; Caraballo et al., 2010; Cortina et al., 2003; Navarro et al., 2006). These latter works do not however, provide complete design models for the engineering application of MgO treatments. Courcelles and co-workers estimated the longevity of PRBs using MgO column laboratory experiments,

coupling chemical reactions and principles of transport in porous media and incorporating system pore volume evolution due to precipitation (Courcelles et al., 2011). Due to the treatment context, their work focused on the impact of permeability reduction on hydraulic conductivity, rather than on maintaining target effluent concentrations. The authors point out that there are several model formulations that consider column porosity loss but neglect the evolution of SSA. In doing so, these approaches underestimate the loss of permeability caused by changes in pore geometry. It was therefore proposed that modeling SSA is essential to understanding the precipitation-clogging phenomenon, and that this factor can be included using the Kozeny-Carman equation in conjunction with the floating spheres model (Courcelles et al., 2011). Although the aim of the above lab and pilot scale studies were to implement an MgO passive low-flow treatment for AMD or contaminated groundwater, the authors monitored and successfully simulated parameters equally important to the drinking water area such as pH, divalent metal retention, the evolution of magnesium and calcium concentrations and changes in column permeability.

Hasson, Schwartz and co-workers investigated the remineralization of desalinated waters with MgO pellets in pure water or waters acidified with CO_2 and H_2SO_4 (Hasson et al., 2013; Schwartz et al., 2015). While both of their models were able to simulate measured Mg^{2+} addition, they did not address the operational lifespan of the column beyond the immediate remineralization demands. Both models consider the kinetics of MgO dissolution to be mass transfer controlled. The modification of the dissolution expression in acidified solutions is not included in Table 2, but can be found in greater detail in Schwartz et al (Schwartz et al., 2015).

Notably, only one model (Courcelles et al., 2011), incorporated the change in reactivity of a column due to the evolution of particle porosity and specific surface area. However, based on work done previously investigating the hydration of MgO, the transient behaviour of MgO particle porosity could have a significant effect on the hydration and the passivation of media.

Table 2.2 Models of MgO in water treatment applications.

Author	***Modeled Phenomenon***	***Validation***
	Dissolution in water	
1, 3	$r = 10^{-4} \cdot a_{H+}{}^{0.45} mol \cdot m^{-2} \cdot s^{-1}$ $m = A\, r(1 - \Omega)$	A, B
4,5	$\frac{C_2}{C_s} = 1 - \exp\left(-\frac{K \cdot a \cdot Z}{L}\right)$ $r = \frac{Q \cdot d[Mg_T]}{dS_p} = k\{[Mg_T]_e - [Mg]\}$ $ln\frac{[Mg_T]_e - [Mg_T]_L}{[Mg_T]_e - [Mg_T]_0} = \frac{6k}{\emptyset} \cdot \frac{(1-\varepsilon)}{d_p} \cdot \tau$	B
	Particle evolution and passivation	
1	$A = A_0 (V\ /\ V_0)^{2/3}$	None
	Contaminant removal	
1, 3	$\frac{-d[Mn^{2+}]}{dt} = k'_1[O_{2(aq)}][OH^-]^2[Mn^{2+}] + k'_2[O_{2(aq)}][OH^-]^2[MnOx][Mn^{2+}]$	A, B
2	$\frac{\partial q}{\partial t} = A \cdot e^{-\left(\frac{E_a}{RT}\right)} = \Pi_i a_i^{\eta_i}(1 - \Omega^p)^q \cdot Sv$	B
	Permeability and hydraulic conductivity loss	
2	$k = \frac{\emptyset^3}{\tau \cdot (1-\emptyset)^2 \left(\sum_{i=1}^{N_m} \frac{\varphi_i}{r_i}\right)^2}$ $\emptyset = 1 - \sum_{i=1}^{N_m} \varphi_i$	C

[A]Verified by mineralogical analysis (XRD) or (EPMA)

[B]Verified by tracking the evolution of dissolved constituent concentrations

[C]Verified by recording differential pressure measured along the depth profile

[1](Tobias S. Rötting et al., 2008), [2](Courcelles et al., 2011) , [3](Macías et al., 2012), [4](Hasson et al., 2013), [5](Schwartz et al., 2015)

To summarize, the four main phenomena listed above are collectively addressed by the design models in Table 2.2; however, none specifically target both the simultaneous remineralization and metal removal capacity of the media which is of interest for drinking water applications. Their validation is therefore currently limited to either permeability loss, remineralization or metal removal breakthrough when modelling long term operation. While not yet adapted to MgO media, Pourahmad and co-workers investigated $CaCO_3$/MgO blends in drinking water treatment and successfully validated manganese removal and remineralization via PHREEQC for a pure calcite column (Pourahmad et al., 2019). Importantly, this work suggests that although media coating eventually passivates the grains in terms of hardness and alkalinity release, this same coating improved metal removal due to the autocatalytic sorption of manganese by MnO_x (Pourahmad et al., 2019). This illustrates the need to further investigate the modelling of media evolution over time when aiming to maintain both hardness addition and metal removal objectives.

2.6.5 Costs

Costs associated with post-treatment are site-specific, and vary depending on the target effluent quality, as well as the technology chosen and the additional costs of consumables. Importantly, the cost-effectiveness of implementing an MgO column is directly linked to its operational longevity. This aspect further emphasises the importance of the design models discussed above. Currently, NSF/ANSI Standard 60 certified magnesium oxide media retails at slightly higher cost (5.73 US$/kg) than calcite (4.44 US$/kg) and dolomite (5.38 US$/kg) per 50 lbs.

2.7 Discussion and suggestions for further research

It is worth mentioning that this review relies on some work outside the drinking water literature, due to the surprisingly limited research concerning MgO in drinking water applications, despite being a common media used in the industry. Accordingly, it would be important to confirm that the phenomenon and performance described by authors working with scenarios of high contaminant concentrations are applicable to the lower concentrations found in drinking water systems. Furthermore, several of the above studies were performed at laboratory scales in controlled environments, a degree of discrepancy between theory and practice must therefore be expected.

Validated design models assist in the application of treatments in real-world context. In this sense, it becomes especially important that MgO dissolution theory is effectively translated to engineering applications. The following section discusses aspects which we believe could be strengthened by further investigation, particularly concerning MgO application for the removal of regulated contaminants.

The models discussed in section 2.3 are derived from MgO dissolution theory outside of the water treatment realm. It should be noted that in what little literature could be found on MgO in drinking water treatment, the kinetic of the media dissolution is most often treated as a simple mass transfer process. While measurements of granular MgO dissolution are shown to be in excellent agreement with values predicted from such a kinetic model (Hasson et al., 2013; Shemer et al., 2015), it cannot adequately predict the longevity of the system if we suppose that the transient behaviour of the porosity of MgO and the passivation of its surface are two important factors influencing dissolution kinetics over time. Although it is noted by several authors and incorporated into the design model presented by Courcelles et al (2011) for an *in situ* GW treatment application, this aspect requires more attention in drinking water applications. The evolution of MgO media reactivity is integral to the operational lifespan of the treatment, not only regarding cost but in order to guarantee effective treatment. If installed domestically for metal removal, without being subject to the same rigour of process control available at the municipal level, early media passivation could lead to the unintended consumption of drinking water which has close to pre-treatment contaminant levels. Furthermore, the longevity of metal retention in an MgO system remains unclear. We know for example that the leaching of metals is pH dependent, and while the metal hydroxides precipitated in the treatment process should remain stable within the pH range 9–11, a decline in media reactivity over time could result in the release of previously removed contaminants as the system pH decreases. Therefore, it is essential that we determine the dominant process responsible for the removal and retention of divalent metals when working with MgO in the context of soft water remineralisation. Considering that MgO is commonly paired with $CaCO_3$ in the industry for remineralisation and pH correction, the impact of equilibrium dynamics in a mixed system is of particular interest and should be investigated in greater detail regarding effluent stability.

2.8 Conclusion

The use of MgO is not novel to the water treatment industry, however this review aimed to provide a synthesis of its uses and potential specific to the drinking water domain. It becomes clear that the advantages of using MgO are numerous, due to its:

- quick hydration and the low solubility of $Mg(OH)_2$ which provides a long-term source of alkalinity and Mg^{2+};
- higher solubility than calcite;
- pH buffering range and ability to retain divalent metal contaminants as compact hydroxide and oxide precipitates;
- health benefits which have been associated with magnesium.

It appears however that very little work has been done to investigate the use of MgO as a simultaneous treatment for remineralization and metal removal, an application which has recently been put forward for $CaCO_3$ contactors. The potential of the media to this regard is significant and warrants further exploration.

Funding: This work was supported by the NSERC Discovery Grant.

CHAPTER 3 RESEARCH OBJECTIVES, HYPOTHESES AND METHODOLOGY

3.1 Objectives and hypotheses

3.1.1 General objective

To investigate the contribution of MgO in a mixed $CaCO_3$/MgO contactor concerning the simultaneous removal of Mn and increase in hardness of treated water during long term operation.

3.1.2 Specific objectives

1) To study the effect of the $CaCO_3$/MgO ratio in a mixed filter on the dissolution kinetics of the media;
2) To compare the Mn removal kinetics of fresh and used $CaCO_3$ and MgO;
3) To determine the relative importance of sorption vs. precipitation in Mn removal by MgO;
4) To evaluate the effect of precipitation nuclei on the removal kinetics of Mn.

3.1.3 Research hypotheses

1) MgO dissolution does not excessively inhibit $CaCO_3$ dissolution;
2) Introducing MgO therefore extends the remineralization capacity of a calcite contactor;
3) The addition of MgO accelerates and increases the removal of Mn;
4) The Mn oxides produced in a mixed media filter are stable and will not be released following a modification of the influent characteristics.

3.2 Methodology

This work was based on two experimental phases which contributed to the investigation of the long-term operation of a $CaCO_3$/MgO contactor :

1) continuous sorption-dissolution column experiments at pilot-scale,
2) batch test experiments investigating the effect of Mn-loading on subsequent Mn removal.

This approach was based on previous work done by Pourahmad and co-workers, and continues the investigation of the operational longevity of a mixed media contactor (Pourahmad et al., 2019). The following sections elaborate the experimental protocol of each phase.

3.2.1 Continuous sorption-dissolution column experiments with mixed media

3.2.1.1 Synthetic feed water (SFW) characteristics

The synthetic feed water (SFW) was prepared by dilution of a stock solution (1000 mg Mn/L) which allowed for the use of a larger quantity of solute and facilitated a more accurate preparation of the desired concentrations for this study. The stock solution was prepared by dissolving powdered reagent grade (>99% pure) $MnSO_4$ (Fisher Scientific, NJ, USA) in ultra-pure (Milli-Q^{TM}) water. Both the stock solution and SFW were found to be stable at a pH of around 6. The SFW was maintained at room temperature (23 ± 2ºC).

3.2.1.2 Media characteristics

A preliminary survey of NSF 60 approved media for drinking water applications identified five major calcite suppliers, while certified magnesia is currently only produced by one supplier. Of these, $CaCO_3$ was purchased from Imarys Marble Inc (Sahuarita, AZ, USA) and MgO from Clack Corporation (Windsor, WI, USA).

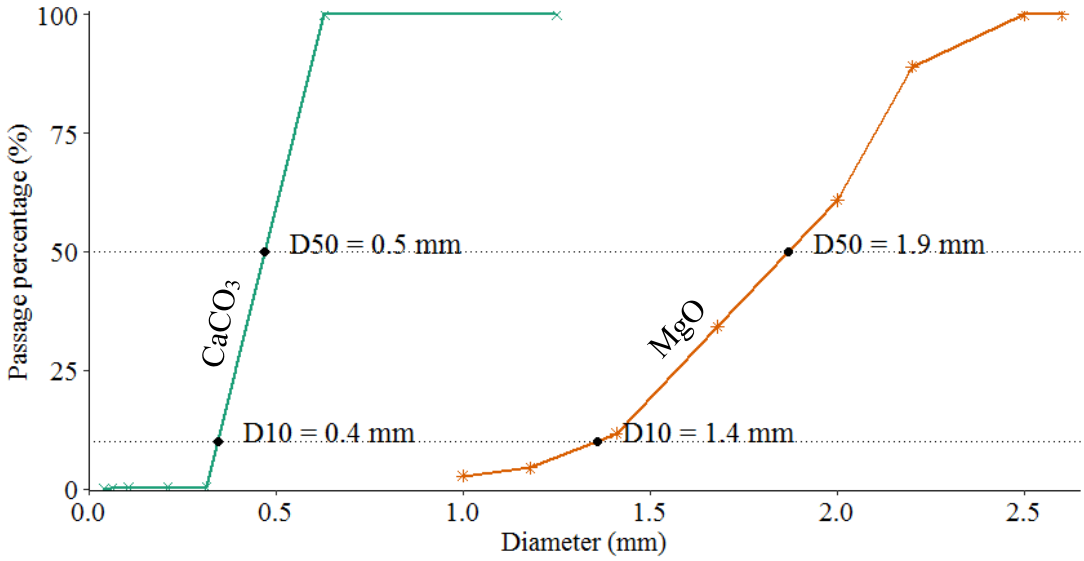

Figure 3.1 Grainsize distribution curves for $CaCO_3$ and MgO media.

Figure 3.1 illustrates the particle size distribution of both media following sieving analyses. As the calcite sand is highly homogeneous, the median (D_{50}) value is close to the effective grain size (D_{10}) reported by the supplier (table 3.1).

Table 3.1 Characteristics of $CaCO_3$ and MgO used in the study.

Filter media	**$CaCO_3$**	**MgO**
Manufacturer	Imarys Marble Inc	Clack Corporation
US mesh size	16 x 40	16 x 6
D_{50}(1) (mm)	0.6	1.9
D_{10}(1,2) (mm)	**0.4**	**1.4**
Purity(3) (%)	99.7	97
Specific gravity(2) (g/cm^3)	2.7	3.6
Bulk density(2) (kg/m^3)	1500	1200
Porosity(2) (ε)	0.42	NA
Surface area(4) (m^2/g)	0.371	0.390
Other impurities(2) (% weight)	0.3 % Mg	0.4 % Fe 1.1 % Ca

(1) Measured in laboratory by sieving analysis.

(2) Provided by supplier.

(3) Determined by ICP-OES (model iCAP 6000, Thermo Instruments Inc) after HNO_3 acidification (Pourahmad et al., 2019).

(4) Data provided via BET measurement from (Pourahmad et al., 2019) using procedure as described in (Gambou-Bosca & Bélanger, 2016)).

For MgO the grain size fraction of 1.2-1.6 mm was used in the experimental process in order to further constrain the particle size distribution. This simplifies the particle size range of MgO media

and remains close to the reported D_{10} value. Other media characteristics are summarized in table 3.1.

3.2.1.3 Experimental set-up and procedure

The first experimental phase aimed to assess the performance of a mixed $CaCO_3$/MgO contactor in attaining both remineralization and Mn removal targets. The assays were carried out at room temperature, in two parallel cylindrical acrylic columns (1.3 m height and 31.75 mm internal diameter). Media ratios were pre-mixed by weight (100/0, 90/10 and 80/20). For each ratio, the columns were then filled to a height of 80 cm and fluidized for two hours to evacuate fine particles.

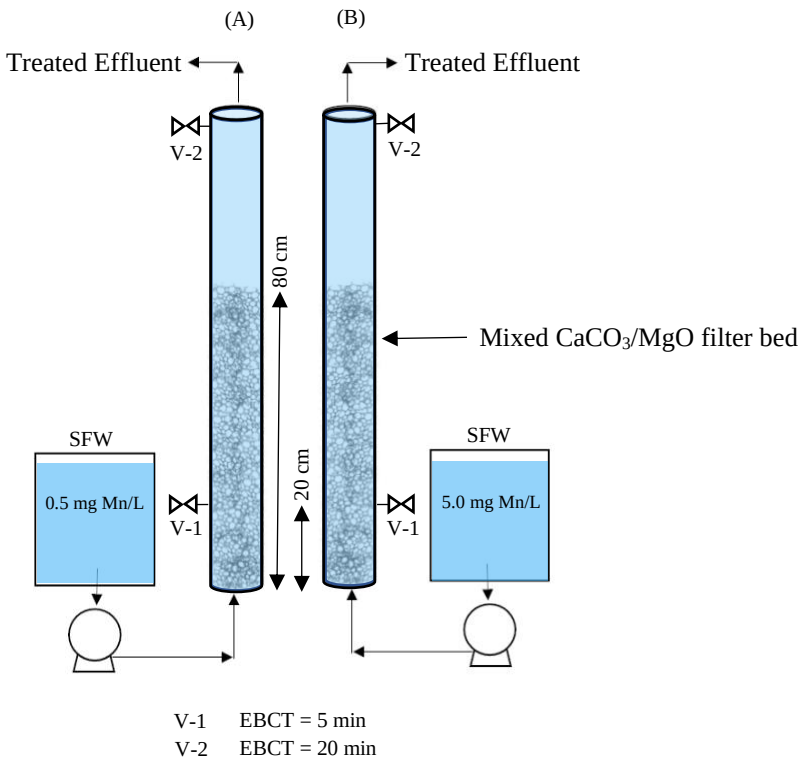

Figure 3.2 Schematic of laboratory column installation.

After washing, the contactors were fed continuously with SFW containing 0.5 mg Mn/L in column A and 5 mg Mn/L in column B. The flow rate was set at 31.5 ml/min, which translates to an upflow velocity of 2.27 m/h and an empty bed contact time (EBCT) of 20 minutes at the effluent. EBCT

is a measure of the time that the water is in contact with the media in the contactor, and is calculated using the following equation :

$$EBCT = \frac{volume\ of\ the\ filter\ bed}{flow\ rate} = \frac{V_B}{Q} \qquad (13)$$

A schematic of the column installation is illustrated in Figure 3.2. It should be noted that the sampling regime of this column design was limited by the low flow rate. In future work, further sampling throughout the column depth (i.e., at 80 cm bed height) could provide additional insights into the reaction progression and would require increasing the flow rate while adapting the contactor dimensions to produce an appropriate EBCT.

Each of the media ratios was initially tested for 72 hours, upon which the ratio 95/5 was implemented for a 720-hour installation to observe the column operation over longer term. For all ratios, samples were collected by syringe at regular intervals from both columns at 5- and 20-minute EBCT. Each sample was analyzed to determine pH (Electrometric Method 4500-H+ B), DIC (GE TOC Analyzer) and alkalinity (Standard Method 2320 B) immediately after collection. Manganese concentrations were also periodically verified by the porphyrin colorimetric method (T(4-CP)P). A duplicate of each sample was stabilized by acidification for later ICP-MS analysis of calcium, magnesium, and manganese concentrations. Total hardness was then calculated using the measured concentrations of dissolved calcium and magnesium (Calculation Method 2340 B).

3.2.1.4 Continuous desorption experiment

Following 720 hours of operation, both columns operating at a ratio of 95/5 were switched to operate with ultra-pure water feeding for 72 hours at the same flow rate. Sampling and measurements proceeded as previously to determine the desorption rate of manganese. The flow rate was periodically monitored at the exit of the column. As previous experiments did not

3.2.1.5 Characterization of Mn-loaded media

Following the operation of the sorption-dissolution columns, used media was collected from a range of column depths for surface analysis using Scanning Electron Microscope (SEM), Energy Dispersive X-ray Analysis (EDX) and X-ray Photoelectron Spectroscopy (XPS). These analyses served to characterize the media after Mn-loading in order to compare the nature of the deposits on the MgO surfaces to those found on calcite. The quantity of Mn-loading was determined by

digesting 1 g of pre-weighted rinsed, dried media (Standard Method 3050B) by progressive heating and the addition of HNO_3 and HCl. Manganese concentrations were measured using ICP-MS following the digestion.

3.2.2 Batch sorption experiments on Mn-loaded media

The effect of Mn-loading on media dissolution and sorption was investigated using batch experiments at 23 ± 2ºC. The batch tests were operated with 10 g/L of Mn-loaded media and were flushed with N_2 gas before being closed to the atmosphere. Tests were repeated using 420 mL of increasing aqueous manganese concentrations (0.0, 0.1, and 1.0 mg Mn/L) and were continuously shaken at 175 rpm for a duration of 48 hours. Samples were taken by syringe at 0.25, 1, 8, 24 and 48 hours and were analyzed to determine pH, DIC, alkalinity, Mn, Ca, and Mg using the same methods as described previously for the column experiments. Additionally, pH and DO were measured continuously inline to capture the rapid pH response upon introduction of the media to the solution, and to monitor the effect of DO on MnO_x species.

3.2.2.1 Negative control batch tests

To investigate the impact of pH on Mn removal, the batch tests were repeated without the addition of media. Instead, the solution pH was manipulated using increasing volumes of 0.01 M Na_2CO_3 to reach target values as summarized in table 3.2. These tests were run for 90 minutes, sampling at 5, 10, 20, 60 and 90 minutes. In addition to continuous pH and DO measurements, the samples were analyzed for DIC and dissolved manganese.

Table 3.2 Volume of buffer required to increase solution to target pH.

Target pH	0.01 M Na_2CO_3 (mL)	Na_2CO_3 Dosage (mg $CaCO_3$/L)
7.0	0.40	0.95
8.0	0.62	1.50
9.0	1.30	3.08
10.0	6.75	16.01

CHAPTER 4 RESULTS

This study was comprised of two experimental phases which investigated the role of MgO in the simultaneous remineralization and removal of manganese from soft waters. The results of continuous sorption-dissolution and batch test experiments are presented and discussed below.

4.1 Continuous sorption-dissolution experiments

In the following sections, column experimental results are presented by parameter (pH, alkalinity, DIC, hardness and dissolved Mn measurements). Unless otherwise indicated, the discussion refers to effluent measurements, which correspond to an EBCT of 20 minutes.

4.1.1 Impact of MgO ratio

The results of increasing the ratio of MgO in a mixed $CaCO_3$/MgO contactor are presented in this section. MgO media is cited in the industry as neutralizing up to 5 times more acidity than $CaCO_3$. This is initially confirmed when observing the pH response, which increases with the ratio of MgO such that the column operating with a 20% MgO produces the highest pH effluent. Over 72 hours of operation, the pure calcite column produced an effluent of pH 9.3-9.8, whereas the columns containing 10 and 20% MgO produced effluents of pH 11.0-11.2 (Figure 4.1a) which exceeds the Health Canada recommended maximal pH of 10.5 for potable water. Further investigation of the impact of MgO content on effluent alkalinity and DIC (mg $CaCO_3$/L) revealed a significant contribution to the stabilization of the soft water feed. While the pure $CaCO_3$ contactor introduced the highest DIC concentrations (approaching 15 mg $CaCO_3$/L), increasing MgO content increased total effluent alkalinity (Figure 4.4b and c). Considering alkalinity to be the sum of $[HCO_3^-]$, $[CO_3^{2-}]$ and $[OH^-]$ species, we might attribute this increase to the presence of a significant fraction of hydroxide alkalinity due to high pH[1].

[1] A pH = 11 implies a concentration of OH^- = 1 meq/L = 50 mg $CaCO_3$/L of alkalinity

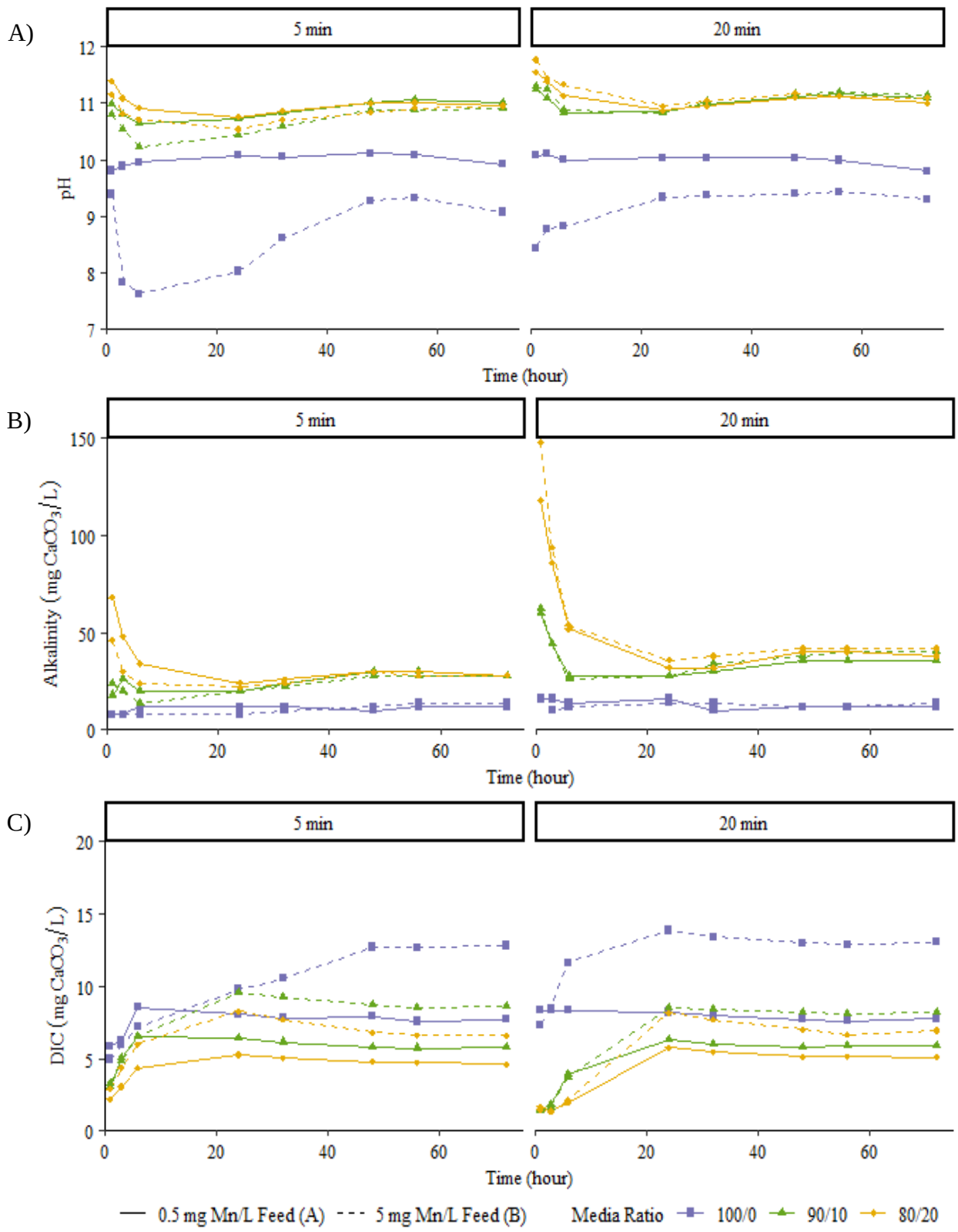

Figure 4.1 Evolution of pH, alkalinity and DIC over 72 hours (23 ± 2 °C). Samples were taken at 20 cm column depth (5 min EBCT) and at the effluent (20 min EBCT).

The dissolution of $CaCO_3$ and MgO media also introduced Ca^{2+} and Mg^{2+} hardness, respectively. Although remineralized, the effluent produced by a pure calcite contactor did not consistently achieve the target total hardness of 30 mg $CaCO_3$/L. Upon the introduction of MgO, mixed media columns resulted in the successful remineralization above target levels (Figure 4.2).

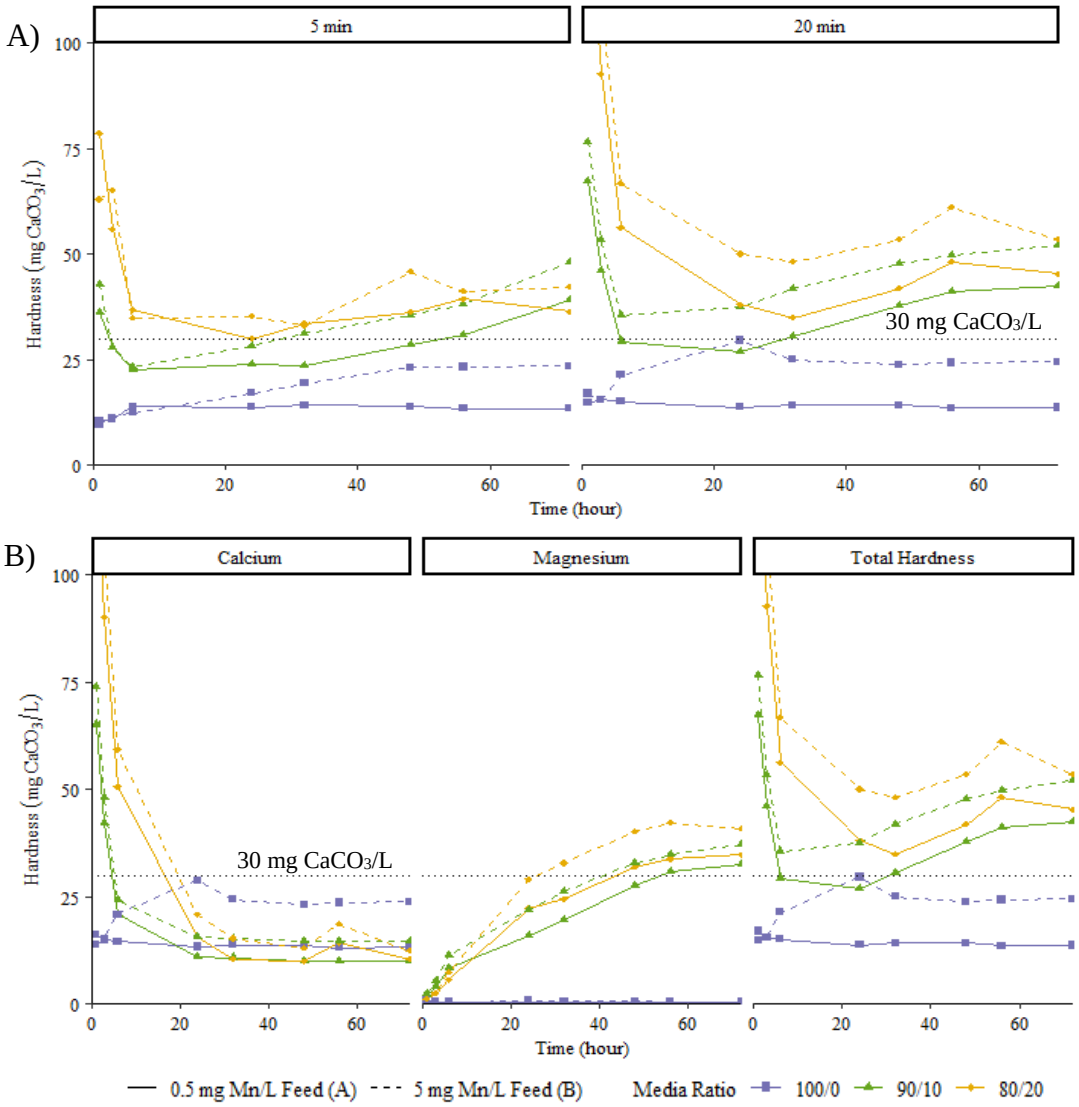

Figure 4.2 Evolution of A) total hardness addition and B) calcium and magnesium hardness contribution at the effluent over 72 hours (23 ± 2 °C). Samples were taken at 20 cm column depth (5 min EBCT) and at the effluent (20 min EBCT).

Although increasing the MgO ratio from 10 to 20% resulted in a distinct hardness spike at the beginning of operation, both ratios produced an effluent hardness of around 50 mg $CaCO_3$/L after 72 hours. This 'spike' is also reflected in the alkalinity, and to a lesser extent, the pH data seen

previously in Figure 4.1. Notably, the curves representing a pure calcite contactor did not exhibit the same trend. We might therefore expect these initial high values to be the result of MgO impurities, such that pH, alkalinity, and hardness are controlled by a small percentage of more soluble fractions (i.e., CaO) at the beginning of column operation. A similar observation was made by Rötting and co-workers, who documented a pH spike above 12 before decreasing to 11 using a column containing 25% MgO (Tobias S. Rötting et al., 2008). During this initial column 'flushing', the difference between MgO ratios is most apparent, as increasing the MgO content increases column impurities. However, after 24 hours the column containing 20% MgO produces an effluent with similar or only slightly higher total hardness measurements as the column operating with 10% MgO.

The addition of MgO also accelerated Mn removal kinetics such that effluent manganese concentrations are reduced to below 0.02 mg Mn/L within the first hour of operation (Figure 4.3). However, increasing the MgO content from 10 to 20 % did not appear to significantly impact removal; both ratios consistently removed up to 99% of dissolved manganese at the effluent. The delay which can be seen for the pure calcite column appears to be further impacted by the influent manganese concentration and is addressed in the following section.

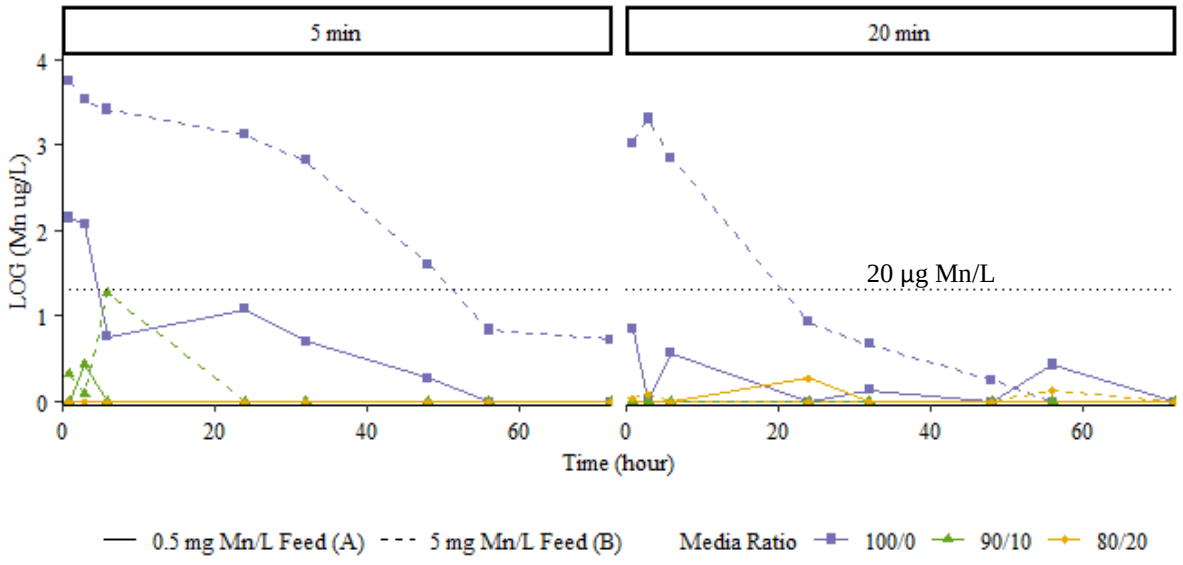

Figure 4.3 Manganese removal in 72-hour column experiments (23 ± 2 °C). Samples were taken at 20 cm column depth (5 min EBCT) and at the effluent (20 min EBCT).

4.1.2 Impact of influent Mn concentration

To investigate the impact of influent Mn concentration on the performance of the mixed media contactor, all column experiments were performed with two feedwater concentrations. As both feedwaters were prepared with ultra-pure water, they contained negligible influent alkalinity and hardness levels, with an initial pH of ~ 6. Column A was consequently fed with 0.5 mg Mn/L, and column B with 5.0 mg Mn/L.

In general, the pure calcite contactor appeared to be most impacted by influent Mn concentrations. This is most apparent in the evolution of pH and DIC measurements over 72 hours, where the higher concentration feed produces a lower pH effluent and higher DIC concentrations. Calcium hardness measurements (Figure 4.2b) further confirm that the calcite media experiences higher dissolution rates in the pure column when compared to treating high influent Mn concentrations with mixed media.

For both tested conditions, all media ratios were able to remove dissolved Mn to below 0.02 mg Mn/L. Again, increasing the influent Mn concentration ten-fold impacted the removal kinetics of the pure calcite contactor most significantly, requiring 24 hours to achieve target Mn removal when treating the 5 mg Mn/L feed. Contactors containing fractions of MgO were able to reduce both influent concentrations to below target levels within the hour which suggest that the high pH favored a higher kinetic or a different mechanism of action (i.e., direct precipitation vs sorption on preformed MnO_x deposits).

4.1.3 Impact of EBCT

To maximize remineralization, the dissolution reaction must reach equilibrium before leaving the bed. For remineralization purposes, the recommended EBCT for a calcite contactor ranges from 10 to 30 minutes (Voutchkov, 2012). As stated in the previous section, our work shows that in mixed media columns, an EBCT of 20 minutes is sufficient to produce an effluent which achieves the treatment target values for the duration of the test. The progression of remineralization and Mn removal can be seen when comparing the effluent water quality with measurements taken closer to the entrance of the column at an EBCT of 5 minutes.

Apart from the higher Mn concentration feed for a pure $CaCO_3$ column, EBCT did not appear to have a significant impact on pH or DIC. This suggests that the dissolution of media at the entrance

of the column rapidly ‘corrects’ the pH of the soft influent water. In practice, it is recommended to adjust the contactor flow conditions such that the EBCT is reduced, and pH over-correction is avoided when using MgO. However, the experimental results indicate that the mixed media columns already ‘over-correct’ pH by 5 minutes of EBCT.

Upon closer investigation, alkalinity measurements exhibited an increase of up to 50% from 5 minutes of EBCT to the effluent measurement of mixed media columns. In contrast, if we associate the carbonate alkalinity contribution with the dissolution of calcite and therefore the introduction of calcium ions into solution, we see both measurements vary minimally from an EBCT of 5 to 20 minutes. One possible explanation for this is that calcite dissolution is most significant at the entrance of the column prior to the increase in pH, whereas the progression of the dissolution reaction for MgO is less impeded by the high column pH after 5 minutes of EBCT. Based on the literature review performed for this work, it was expected that a mixed media column would be unable to attain equilibrium for both minerals. Inevitably, the mixed media column will produce a water which is under-saturated with respect to either $CaCO_3$ or MgO due primarily to the impact of pH on their respective equilibrium dynamics.

4.1.4 Impact of operation time: 30-day experiment

Following the 72-hour column results, the experiment was repeated with a 95/5 media ratio for a duration of 720 hours (30 days) to monitor the impact of Mn-loading on the contactor performance. The fraction of MgO was reduced to 5% to investigate if the pH response could be constrained to a lower pH (i.e., lower than pH 10.5) while still achieving remineralization and Mn removal targets.

Figures 4.4 and 4.5 suggest that while the shorter duration experiments appeared to show a stabilization of effluent measurements within 72 hours, this in fact occurs closer to 96 hours when monitoring water quality over long term operation. Consequently, the impact of influent Mn concentration and EBCT becomes more apparent over 720 hours of operation. Otherwise, the evolution of the treated water quality (pH, alkalinity, DIC) demonstrates the same general trends identified and discussed in the previous sections.

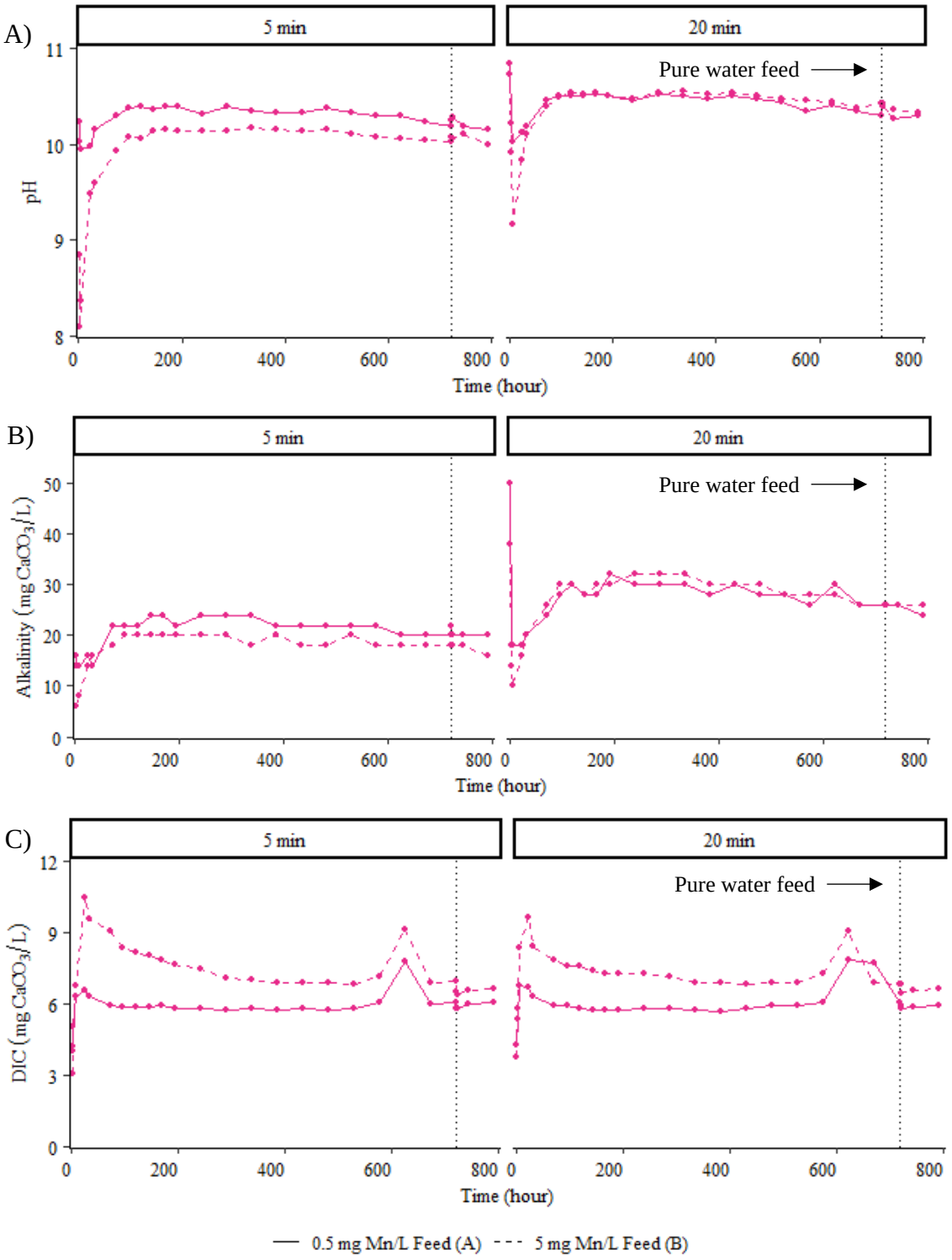

Figure 4.4 Evolution of pH, alkalinity and DIC over 720-hour column experiments using a 95/5 ratio of $CaCO_3$/MgO (23 ± 2 °C). Samples were taken at 20 cm column depth (5 min EBCT) and at the effluent (20 min EBCT).

Following an initial pH spike to 10.8 attributed to the 'flushing' of media impurities, effluent pH was successfully constrained to 10.5 and below for the duration of the test. Effluent hardness remained close to 30 mg $CaCO_3$/L at the end of operation despite a gradual decrease after 144 hours. Figure 4.5b illustrates that this decrease is due to a decrease in aqueous Mg^{2+}, whereas the contribution of the Ca^{2+} to total hardness remains relatively stable throughout the duration of the operation. After switching to an ultrapure water feed, the column which had been treating 5 mg Mn/L experienced an isolated magnesium concentration spike after 24 hours; otherwise, the effluent hardness did not indicate improved dissolution in the absence of influent Mn concentrations.

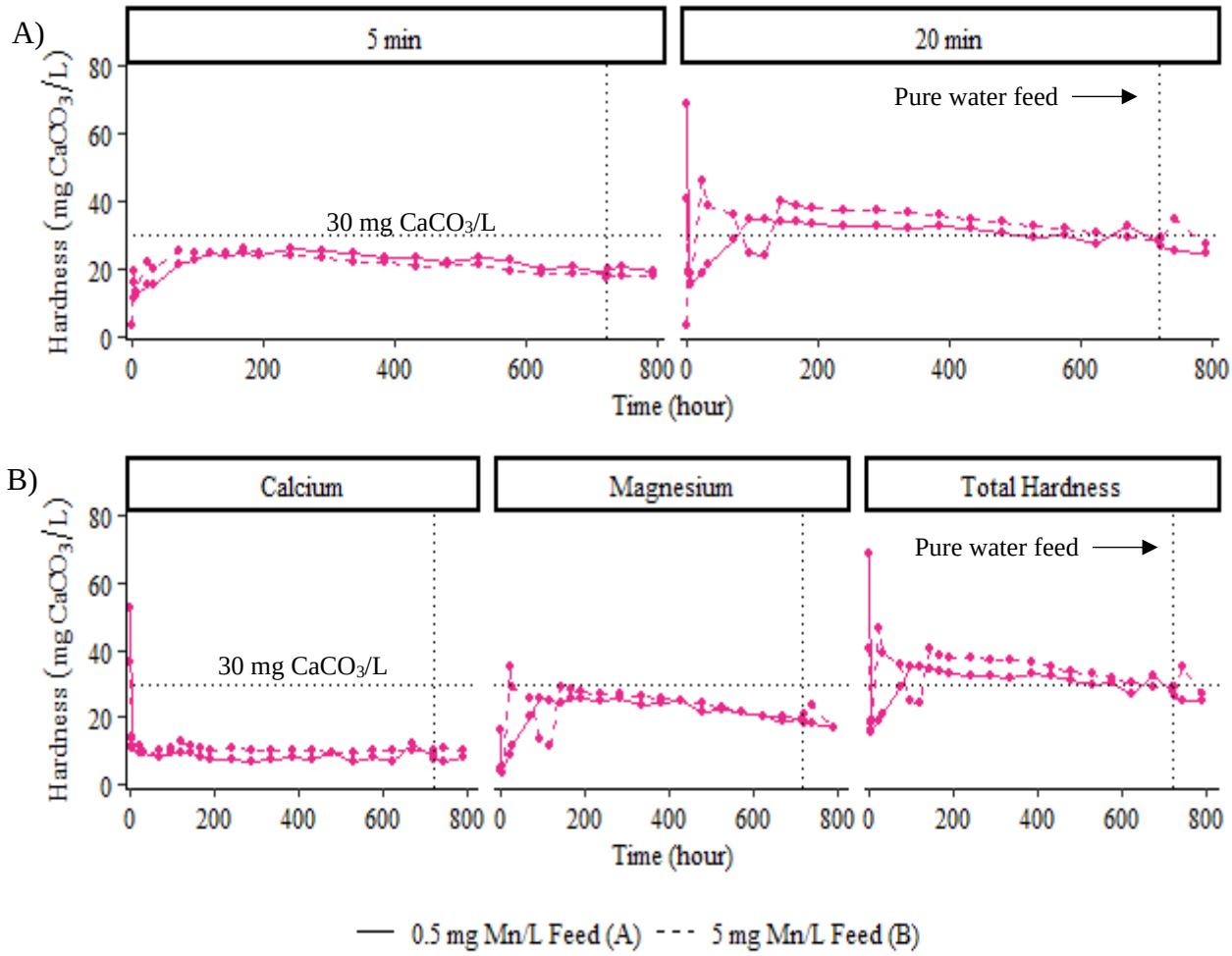

Figure 4.5 Evolution of A) total hardness addition and B) calcium and magnesium hardness contribution at the effluent in the 720-hour column experiments using a 95/5 ratio of $CaCO_3$/MgO (23 ± 2 °C). Samples were taken at 20 cm column depth (5 min EBCT) and at the effluent (20 min EBCT).

This suggests that the Mn-phases present on the used media surfaces contribute to limiting media dissolution over the long-term operation of the contactor.

Aqueous manganese concentrations were reduced to below the target of 0.02 mg Mn/L within 6 and 24 hours for the lower and higher concentration feeds, respectively (Figure 4.7). Again, 99% removal was achieved for both effluents once stabilized, and was maintained for the duration of the experiment. Notably, samples taken after switching to a pure water feed indicated the continued presence of aqueous manganese concentrations. Although these concentrations remain well below the AO, they suggest the possible remobilization of Mn in response to altered feedwater characteristics.

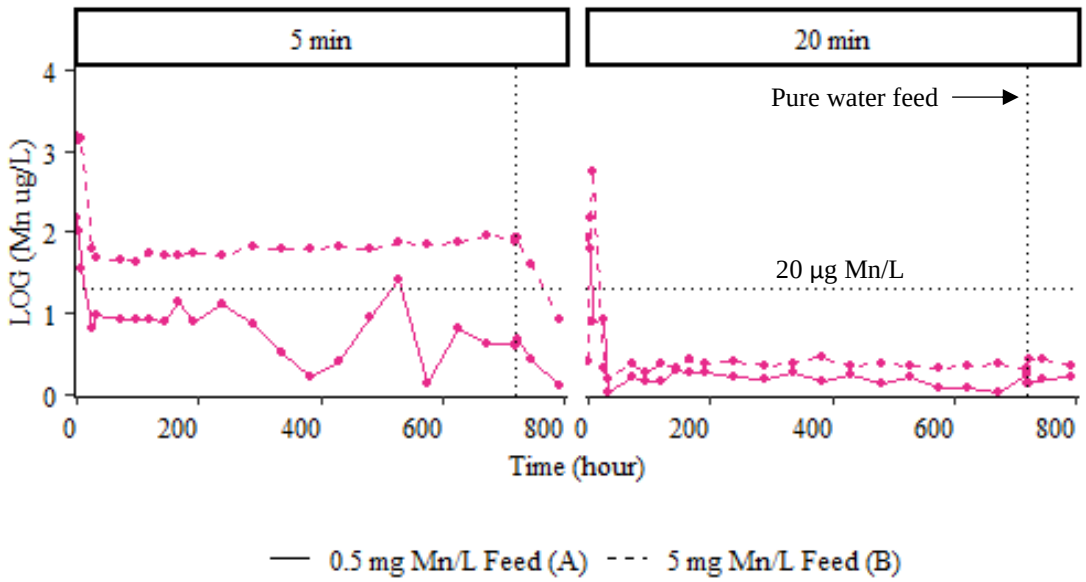

Figure 4.6 Manganese removal in 720-hour column experiments using a 95/5 ratio of $CaCO_3$/MgO (23 ± 2 °C). Samples were taken at 20 cm column depth (5 min EBCT) and at the effluent (20 min EBCT).

The data obtained from the 30-day test confirms that the operation of the mixed media column can maintain relatively stable effluent water quality with as little as 5% MgO. The gradual decline in hardness addition is an improvement to previous work which saw a distinct remineralization breakthrough at 600 hours for a pure calcite column treating 5 mg Mn/L (Pourahmad et al., 2019).

4.2 Media Characterization

Fresh $CaCO_3$ and MgO media were analyzed by SEM, EDX and XPS, as well as after long-term operation of the contactor column with a 5 mg Mn/L influent. In comparison to fresh media surfaces (0 mg Mn/L), we can see that used media surfaces exhibit distinct both crystal growth and precipitates (Figure 4.1). For both media, the decrease in Mn-phases corresponds to samples taken at increasing EBCT, suggesting that Mn-removal occurs primarily at the entrance of the contactor. This corresponds with the colour change that we see in the contactor during operation, where the media at the entrance of the up-flow column turns brown-black. Most manganese oxide minerals are brown-black and identifying the particular mineral can be a challenge. Therefore the more general term of ‘‘Mn oxide’’ or MnO_x is often reported rather than a particular mineral phase (Post, 1999). High resolution XPS analysis confirms the presence of Mn2p spectra which implies the presence of MnO_2, Mn_2O_3 and/or MnO(OH), as seen in Figure 4.8. Mn-loaded surfaces also produce O1s and Mg1s spectra, which correspond to the MgO surface and the crystallization of magnesium carbonates (Table 4.1). Previously, comparable surface analyses of media from a pure $CaCO_3$ column led to the hypotheses that Mn sorption is initiated by an ion exchange reaction between aqueous Mn^{2+} and Ca^{2+} from the $CaCO_3$ matrix, followed by the slow recrystallization of $MnCO_3$ into MnO_2 (Pourahmad et al., 2019). In a mixed media column, we might expect a similar sorption-recrystallization mechanism for $CaCO_3$ media, although the presence of Mg^{2+} in the aqueous phase introduces cation competition for the exchange or sorption of Mn^{2+}. Furthermore, manganese removal using MgO has been suggested to be controlled by the rapid oxidation of Mn^{2+} at high solution pH and subsequent precipitation of Mn^{3+} phases (Caraballo et al., 2010; Cortina et al., 2003; Tobias S. Rötting et al., 2008). pH-based calculations predicted MnO(OH) and MnO_2 phases as oversaturated or close to equilibrium, and Cortina and co-workers successfully identified Mn_3O_4 and MnO(OH) precipitates by XRD (Cortina et al., 2003). Visually, the surface coatings shown in our results (Figure 4.1) indicate that well defined crystals are not only present but increasing with decreasing solid phase Mn concentrations. This suggests that these structures are most likely the Mg-carbonates which are favoured with increasing concentrations of aqueous Ca^{2+}/Mg^{2+}, whereas MnO_x occur as a less well-ordered precipitate mass at the entrance of the column.

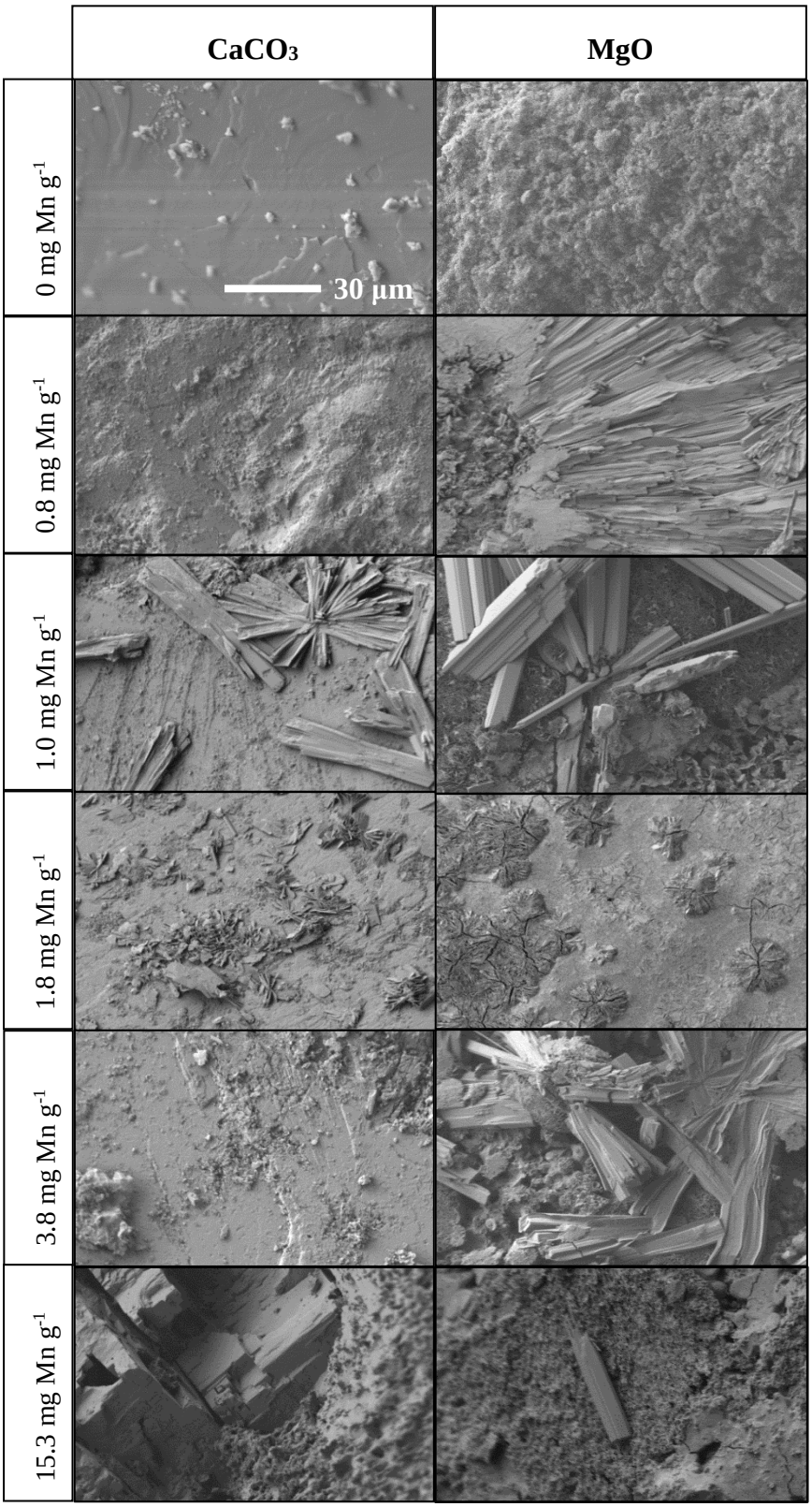

Figure 4.7 SEM images (x 1000 magnification) of Mn-loaded media surfaces.

Table 4.1 High resolution XPS spectra for fresh and Mn-loaded media.

Name	BE (ev)	Identification	Relative atomic %			
			Fresh ≈ 0 mg/g		Mn-loaded 15 mg/g	
			$CaCO_3$	MgO	$CaCO_3$	MgO
C1s	285.0	C-C	ND	17.24	36.4	26.65
	288.7	O-C=O	34.24	ND	ND	ND
	290.1	R-CO_3	ND	ND	34.82	ND
Ca2p	347.3	$CaCO_3$	14.69	ND	9.46	ND
	350.38	$CaCO_3$	ND	10.93	ND	ND
Mg1s	1304.5	MgO	1.22	11.64	ND	10.55
	1305	$MgCO_3$	ND	ND	5.66	ND
O1s	530.5	MeO_x	ND	ND	ND	52.79
	531.9	R-CO_3, Me-OH, Si-O	49.5	54.45	47.1	ND
Mn2p3	641.7	MnO_2, Mn_2O_3 or MnO(OH)	ND	ND	1.39	10

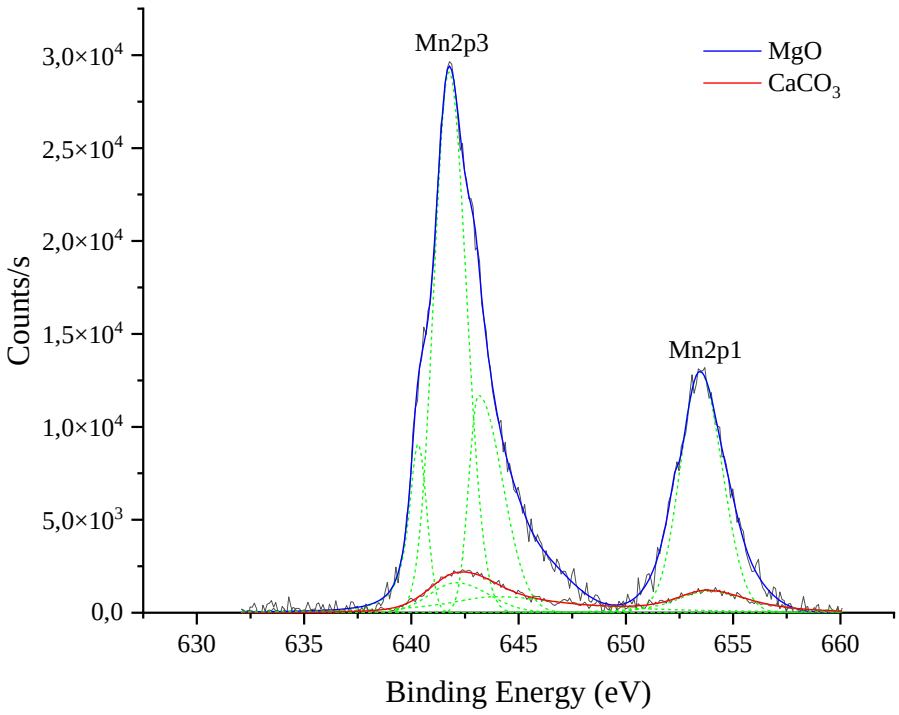

Figure 4.8 XPS analysis of Mn-loaded (15 mg/g sample) MgO in blue and $CaCO_3$ in red for the region of Mn oxides.

4.3 Batch sorption experiments on Mn-loaded media

4.3.1 Mn removal kinetics

Figure 4.9 compares the Mn removal kinetics in a batch reactor containing fresh or Mn-loaded media from 72-hour column experiments. A concentration of 10 g/L of media were added to the batch reactors. The presence of Mn-loading on calcite media (5 mg Mn/g sample) improved the reaction kinetics as well as the removal of Mn from solution. However, both fresh and Mn-loaded **calcite** required longer to attain a stable sorption regime in comparison to fresh MgO or Mn-loaded **mixed media** (5 mg Mn/g sample) which stabilized within an hour. For each batch test, the equilibrium condition is indicated by a red line, with the exception of the Mn-loaded media ratios containing 0-10 % MgO, which share a line as their sorption regimes eventually converged at 8 hours and stabilized at similar removal capacities of approximately 76% (Figure 4.9a). As well,

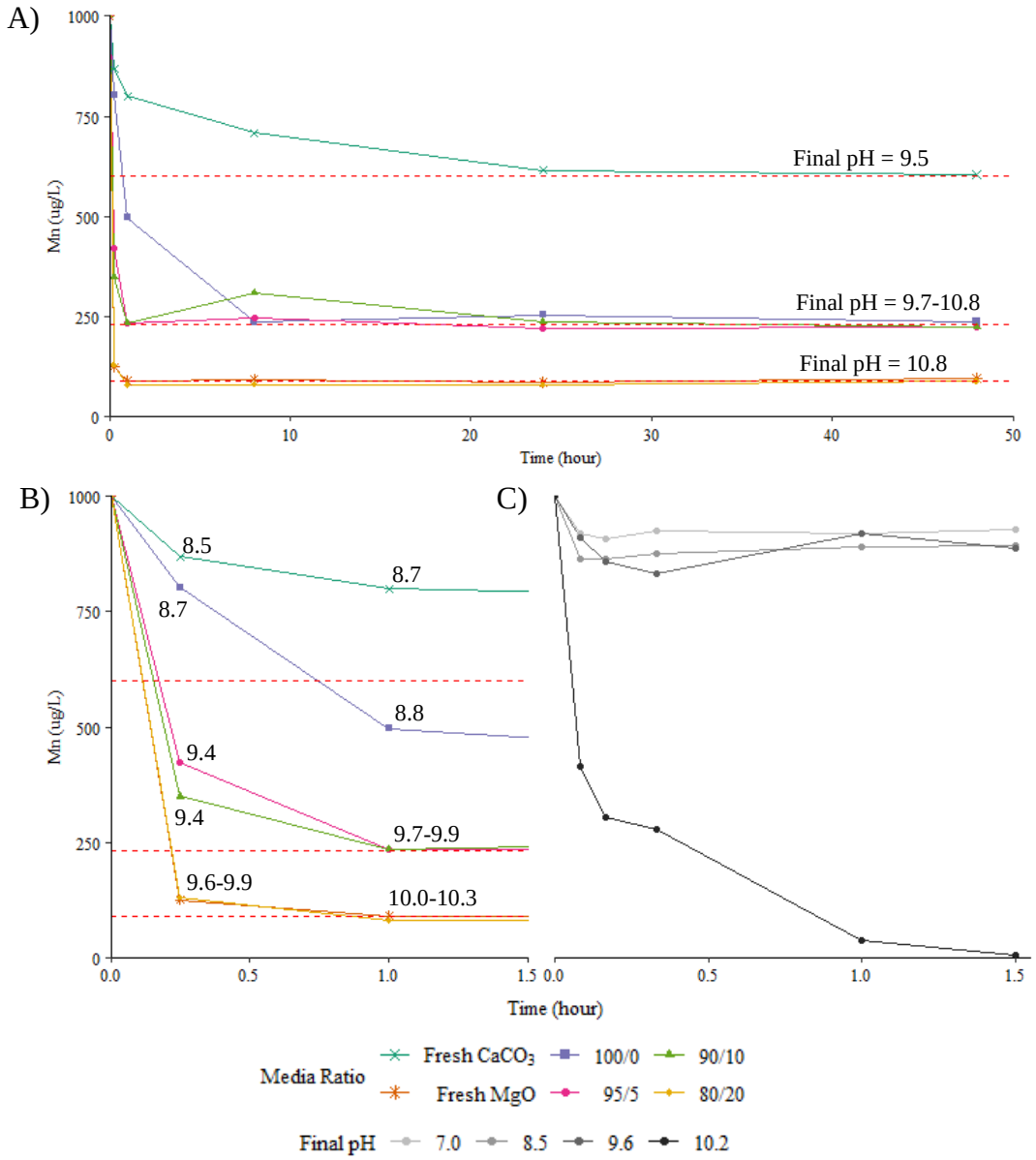

Figure 4.9 A) Impact of solid Mn-phase (5 mg Mn/ g sample) and media ratio on Mn^{2+} removal in batch tests, B) impact of pH evolution (labelled points) leading to stable Mn-removal regimes and C) pH-induced precipitation of Mn in the absence of media (23 ± 2 °C).

Mn-loaded mixed media with 20% MgO showed nearly identical reaction kinetics to fresh MgO in the conditions tested. The convergence of different ratios at 76% removal suggests that the presence of Mn-phases on the used media surfaces may be contributing to long-term Mn removal regardless of varying MgO content. However, the ratio of MgO available for dissolution and the

corresponding increase of solution pH likely remains an important kinetic factor. Figure 4b illustrates that increasing the MgO fraction accelerates the removal of Mn within the first 15 minutes of operation. The impact of MgO on Mn-removal kinetics is discussed further in the following section.

4.3.2 Effect of pH on precipitation of $Mn_{(aq)}$

With the aim of further investigating the effect of pH on Mn removal (concentration = 1 mg Mn/L), a negative control test was performed in which the pH of the batch test solution was increased without the addition of media. Figure 4.9c illustrates that Mn precipitation is minimal within the range of pH 7.0-9.6, but that 99% removal is achieved when the pH is increased to 10.2. In the presence of media (Figure 4.9b), we can therefore assume that pH-induced precipitation from the aqueous phase does not significantly impact Mn removal for either fresh or Mn-loaded $CaCO_3$. In comparison, fresh MgO and the Mn-loaded mixed media containing 5-20% MgO buffer the solution to a final pH which is above 10.2. At these conditions, we would predict an almost complete removal of aqueous Mn by precipitation. Instead, the batch tests stabilize at 90% and 76% removal, respectively. One possible explanation for this is that the introduction of as little as 5% MgO causes the precipitation of a fraction of the aqueous Mn-phase into Mn hydroxide and carbonate particles due to high solution pH, while solid Mn-phase sorption controls removal kinetics once the aqueous phase has been significantly reduced. This partial precipitation mechanism could account for the increased rate of removal seen within the first 8 hours of operation in comparison to pure calcite with the same concentration of solid Mn-phase.

4.3.3 Effect of precipitation nuclei on Mn sorption

As mentioned, the presence of solid Mn-phases on used media surfaces accelerates the rate of Mn-removal in batch tests. For pure calcite, the formation of this coating was found to improve Mn removal due to the autocatalytic nature of the adsorption/oxidation of dissolved manganese by MnO_x (Pourahmad et al., 2019). It is difficult to distinguish if the precipitation of divalent metals as Me-hydroxides occurs as a direct nucleation on the brucite surface (i.e. hydrated MgO surface) or if they are formed within the fluid boundary layer before attaching (Hövelmann et al., 2018). In their work, Hövelmann and co-workers suggested among several possible reaction pathways, the aggregation of metal nanoparticles on the $Mg(OH)_2$ surface and the consequent

crystallization/transformation of these aggregates into a distinct precipitate surface. These precipitation nuclei can then serve to further remove dissolved Me^{2+} species through ion-by-ion growth, or by the sorption of oxidated colloidal particles present in the fluid boundary layer (Hövelmann et al., 2018). In the presence of MgO which rapidly hydrates to $Mg(OH)_2$, we might therefore expect that Mn removal is not only improved due to pH-induced precipitation, but that the removal kinetic is gradually improving during column operation due to the increased presence of precipitation nuclei on both media surfaces. Further experimental work required to confirm this hypothesis is discussed in greater detail in section 5.4.

CHAPTER 5 GENERAL DISCUSSION

This chapter summarizes the main findings of this study and explores the potential of modeling a mixed $CaCO_3$/MgO contactor. The main objective of this research effort was to investigate the contribution of MgO in the simultaneous remineralization and removal of manganese for residential soft waters. Hardness addition and manganese removal targets in treated water were 30 mg $CaCO_3$/L and 0.02 mg Mn/L, respectively. With this aim, the following was investigated:

1) the impact of MgO ratio on achieving target effluent water quality;
2) Mn removal kinetics using fresh and used $CaCO_3$ and MgO;
3) the relative importance of sorption vs. precipitation in Mn removal by MgO;
4) the effect of precipitation nuclei on the removal kinetics of Mn.

5.1 Impact of MgO ratio on Mn removal and hardness adjustment

Week and month long column experiments illustrated that a mixed contactor can achieve effluent water quality targets with as little as 5% MgO content. In fact, higher fractions of MgO 'over-corrected' the pH to above 10.5, which is unfavorable for potable water. It should be noted that being limited to operating with 5% MgO content may require replenishing the filter media multiple times a year, as indicated by the gradual hardness decline over 30 days of operation. It could therefore be of interest to increase the MgO content using a larger grain size fraction of media, such that the reaction surface of the media is decreased, and the pH is still constrained to below 10.5. Importantly, the successful introduction of an MgO fraction into a mixed media column allows for the addition of both calcium and magnesium hardness, which is desirable in drinking water for cardiac health (World Health Organisation (WHO), 2005).

The effect of Mn-loading on the dissolution reaction is inevitable over long-term operation of a contactor. While previous work showed a distinct effluent hardness decline at 600 hours for a pure calcite column due to Mn-loading on media, the addition of 5% MgO appears to mitigate the Mn-loading effect, thereby extending the remineralization capacity of a comparable column. Previously, Pourahmad and co-workers also investigated the Mn desorption rate from Mn-loaded calcite surfaces and found no significant back dissolution of Mn to the aqueous phase; indicating a

stable Mn-phase (Pourahmad et al., 2019). Notably, this Master's work shows a slight remobilization of Mn in effluent samples (max 3 μg Mn/L) taken from Mn-loaded mixed media columns that were switched to an ultra-pure water feed. This is possibly due to the increased importance of Mn-removal by precipitation, as MgO dissolution produces a pH increase which is conducive to the precipitation of $MnCO_3$, MnO(OH) or MnO_x. Although the solubility and surface charge of MgO is known to favor the formation of compact precipitates (Schiller et al., 1984), further investigation is required in order to identify how fluctuating the influent water quality could affect solid Mn-phase stability.

5.2 Mn removal kinetics using fresh and used $CaCO_3$ and MgO

Over 48 hours, batch tests showed that fresh and Mn-loaded calcite (5 mg Mn/g sample) required longer to attain a stable sorption regime in comparison to fresh MgO or Mn-loaded mixed media (5 mg Mn/g sample) which stabilized within an hour. It should be noted that the reaction kinetics identified in the batch tests are expected to be enhanced in the column experiments, which had a significantly more favourable ratio of influent Mn to grams of media and were also able to reduce Mn concentrations by 99%. Nevertheless, Mn-loaded media (0-10% MgO), eventually converge at the same sorption regime after 8 hours, with 76% Mn removal. It therefore appears that while increasing the MgO fraction accelerates initial Mn-removal kinetics, the formation of Mn-phases on the used media surfaces likely remains an important factor in continued Mn-removal during the operation of the column.

5.3 Importance of sorption vs. precipitation in Mn removal by MgO

The removal of dissolved divalent metals by MgO has been cited as a possible sorption-coprecipitation process, where the dissolution of MgO promotes the oxidation of metal hydroxides into negatively charged metal oxides which adsorb Me^{2+} remaining in solution (Balintova & Petrilakova, 2011; Cao et al., 2012; Choi et al., 2014; Hövelmann et al., 2018; Navarro et al., 2006; Tobias Stefan Rötting et al., 2006). Batch test results confirm that at a pH of 10.2, dissolved Mn is nearly completely removed from solution within 90 minutes, even in the absence of media. This suggests that pH-induced precipitation is likely an important mechanism in the Mn-removal reaction occurring in a mixed media contactor, which raises the solution pH up to 10.5 with the

addition of 5% MgO. Indeed, a precipitation step could account for the increased rate of removal which is seen in comparison to pure calcite with the same concentration of solid Mn-phase. The dissolution of MgO should therefore cause the precipitation of a fraction of the aqueous Mn-phase as Mn hydroxides and carbonates due to high solution pH, while solid Mn-phase sorption controls removal kinetics once precipitation nuclei are established and the aqueous phase has been significantly reduced. This combined mechanism is also important to take into consideration for the lifespan of the contactor. If pH-induced precipitation were the primary removal mechanism, the column would likely experience clogging at the entrance where Mn is quickly oxidized, and high precipitation rates could risk cementing the media. As this was not observed in the 30-day column experiment, it is expected that a small percent fraction of MgO favours the sorption-coprecipitation pathway.

5.4 The effect of precipitation nuclei on the removal kinetics of Mn

To better distinguish the role of Mn coating on the removal of aqueous Mn concentrations in a mixed system, it would be necessary to repeat the batch tests with the respective ratios of fresh media (95/5, 90/10 and 80/20) to represent the absence of precipitation nuclei at time zero. It would also be of interest to investigate the impact of increasing the initial precipitation nuclei (i.e., solid Mn-phases) from 5 mg Mn/g media to 15 mg Mn/g media, corresponding to used media from 72 and 720 hours of column operation, respectively. Interestingly, Pourahmad and co-workers previously recorded the same concentration of solid Mn-phase (15 mg Mn/g sample) after treating the same influent concentrations (5 mg Mn/L) for approximately 800 hours with a pure calcite contactor. Without an MgO fraction, another week of operation was required to form a comparable solid Mn-phase concentration. Importantly, the distribution of the solid Mn-phase on used media can currently only be estimated with the results from this work. Both the measured decline of magnesium hardness during 720 hours of operation (Figure 4.5b), as well as XPS analysis of used media from the long-term column experiment (Table 4.1) suggest that the solid Mn-phase is predominantly present on the used MgO surface. In the conditions tested, it therefore appears that MgO may act as the preferred reaction surface for the nucleation and growth of Mn-precipitates in a mixed media system. However, it is unlikely that the distribution of media within the column was perfectly uniform. Furthermore, to the naked eye the MgO particles did not always appear to have the dark coating indicative of MnO_x, even when surrounding calcite grains did (see Appendix A).

The heterogeneity of a mixed media column therefore poses a challenge in quantifying the role of the respective media in Mn-removal. Designing a column which constrains MgO into a distinct layer within the column could be of interest in future work.

5.5 Modeling the long-term performance of a mixed media contactor for Mn-removal and remineralization

As highlighted by the literature review, previous work modeling MgO columns in water treatment research primarily addresses metal removal kinetics, and more rarely the media's remineralization capacity. However, modeling of the pure calcite system is well established. While no model currently exists that is able to predict simultaneous remineralization and metal removal in waters treated with MgO filters, previous work in our laboratory led to the successful calibration of such a model for pure calcite using PHREEQC (Pourahmad et al., 2019). With the experimental data available from this current research, it would be possible to similarly construct a model for the mixed media contactor. Previously, a simple calcite dissolution rate based on the calcite saturation index was defined due to its success in modeling applications of phosphorus precipitation in packed bed contactors (Claveau-Mallet, Courcelles, Pasquier, & Comeau, 2017). The model was then further developed by :

- designating the Mn removal pathway and rate;
- setting the molar repartition of mineral phases present on the used media surfaces, and
- incorporating the effect of diffusion limitation with progressive Mn-loading.

In a mixed $CaCO_3$/MgO system, the reaction pathways are more complicated, as there are more constituents with the potential to interact in the dissolution-precipitation process. However, as discussed previously, a combined sorption-coprecipitation-recrystallization mechanism is expected to govern Mn removal by MgO. Constructing the model's reaction pathway and molar repartition of MnO_x is further informed by surface analyses which measured ~10 times more solid-phase Mn on MgO surfaces than on used $CaCO_3$ media. Achieving a satisfactory reproduction of further experimental data such as pH, Ca^{2+}/Mg^{2+}, total hardness and manganese concentrations would consequently allow for the calibration of the model.

CHAPTER 6 CONCLUSIONS AND RECOMMENDATIONS

This project investigated the contribution of MgO in a mixed media contactor with the aim of improving remineralization and Mn-removal performance over long-term operation. Our results led to the following main conclusions :

• Long-term performance of a mixed $CaCO_3$/MgO contactor

Over 720 hours of operation, the mixed media contactor with a 5% MgO ratio was shown to maintain effluent hardness levels of close to 30 mg $CaCO_3$/L and to remove aqueous Mn concentrations to below 0.02 mg Mn/L. The addition of MgO adds magnesium hardness to the finished water as well as accelerating and improving Mn removal in comparison to treatment with pure $CaCO_3$.

• Importance of precipitation in Mn removal by MgO

The addition of as little as 5% MgO increases the pH up to 10.5, which introduces a significant precipitation mechanism as Mn^{2+} is oxidized. However, batch test results suggest that removal may still be governed by a sorption-coprecipitation reaction, as the stable sorption regime of Mn-loaded mixed media is comparable to that of pure calcite media with the same concentration of Mn coating.

• Stability of the solid Mn-phase

Compared to a pure $CaCO_3$ contactor, the mixed media column showed the remobilization of solid-Mn phases when switched to an ultra-pure water feed after treating up to 5 mg Mn/L for a duration of 720 hours. Although the Mn concentrations remained well below 0.02 mg Mn/L and would not cause aesthetic or health problems, the mixed $CaCO_3$/MgO system is necessarily more complex than that of a pure calcite column and the stability of the solid phases should be further investigated.

The following are aspects of the mixed-media contactor system which we recommend for further investigation :

- develop a model for a mixed $CaCO_3$/MgO column to predict the long-term behavior of the contactor;
- optimize the mixed media contactor design by :
    - investigating the effect of particle size on MgO dissolution with the aim of increasing the MgO fraction without producing an effluent above pH 10.5;

  - investigating the impact of a layered $CaCO_3$/MgO filter;

- explore the treatment capacity of a mixed media contactor for waters with additional contaminant constituents commonly found in residential groundwater sources (i.e., iron);
- evaluate the long-term performance of a mixed contactor in a pilot-scale study using natural groundwater.

REFERENCES

(ATSDR), A. f. T. S. a. D. R. (2012). *Toxicological profile for Manganese*. Atlanta, GA: U.S: Public Health Service.

Amaral, L. F., Oliveira, I. R., Salomao, R., Frollini, E., & Pandolfelli, V. C. (2010). Temperature and common-ion effect on magnesium oxide (MgO) hydration. *Ceramics International, 36*(3), 1047-1054. doi:10.1016/j.ceramint.2009.12.009

Aphane, M. E., van der Merwe, E. M., & Strydom, C. A. (2009). Influence of hydration time on the hydration of MgO in water and in a magnesium acetate solution. *Journal of Thermal Analysis and Calorimetry, 96*(3), 987-992. doi:10.1007/s10973-008-9095-y

Avrami, M. (1939). Kinetics of Phase Change. I General Theory. *The Journal of Chemical Physics, 7*(12), 1103-1112. doi:10.1063/1.1750380

Ayotte, J. D., Gronberg, J. A. M., & Apodaca, L. E. (2011). *Trace elements and radon in groundwater across the United States, 1992-2003* (2011-5059). Retrieved from Reston, VA: http://pubs.er.usgs.gov/publication/sir20115059

Bahadori, A. (2010). Prediction of Scale Formation in Calcium Carbonate Aqueous Phase for Water Treatment and Distribution Systems. *Water Quality Research Journal, 45*(3), 379-389. doi:10.2166/wqrj.2010.038

Balintova, M., & Petrilakova, A. (2011). *Study of pH Influence on Selective Precipitation of Heavy Metals from Acid Mine Drainage* (Vol. 25).

Birchal, V. S., Rocha, S. D. F., & Ciminelli, V. S. T. (2000). The effect of magnesite calcination conditions on magnesia hydration. *Minerals Engineering, 13*(14), 1629-1633. doi:https://doi.org/10.1016/S0892-6875(00)00146-1

Birchal, V. S., Rocha, S. D. F., Mansur, M. B., & Ciminelli, V. S. T. (2002). A simplified mechanistic analysis of the hydration of magnesia. *Canadian Journal of Chemical Engineering, 79*(4), 507-511.

Birnhack, L., Voutchkov, N., & Lahav, O. (2011). Fundamental chemistry and engineering aspects of post-treatment processes for desalinated water—A review. *Desalination, 273*(1), 6-22. doi:https://doi.org/10.1016/j.desal.2010.11.011

Blesa, M. A. (1994). *Chemical Dissolution of Metal Oxides*. Boca Raton: CRC Press.

Bouchard, M. F., Sauvé, S., Barbeau, B., Legrand, M., Brodeur, M., Bouffard, T., . . . Mergler, D. (2011). Intellectual impairment in school-age children exposed to manganese from drinking water. *Environ Health Perspect, 119*(1), 138-143. doi:10.1289/ehp.1002321

Bratton, R. J., & Brindley, G. W. (1965). Kinetics of vapour phase hydration of magnesium oxide. Part 2.—Dependence on temperature and water vapour pressure. *Transactions of the Faraday Society, 61*(0), 1017-1025. doi:10.1039/TF9656101017

Brown, G. E., Henrich, V. E., Casey, W. H., Clark, D. L., Eggleston, C., Felmy, A., . . . Zachara, J. M. (1999). Metal Oxide Surfaces and Their Interactions with Aqueous Solutions and Microbial Organisms. *Chemical Reviews, 99*(1), 77-174. doi:10.1021/cr980011z

Buhmann, D., & Dreybrodt, W. (1985). The kinetics of calcite dissolution and precipitation in geologically relevant situations of karst areas: 1. Open system. *Chemical Geology, 48*(1), 189-211. doi:https://doi.org/10.1016/0009-2541(85)90046-4

Cahn, J. W. (1956). The kinetics of grain boundary nucleated reactions. *Acta Metallurgica, 4*(5), 449-459. doi:https://doi.org/10.1016/0001-6160(56)90041-4

Canada, H. (2019). *Guidelines for Canadian Drinking Water Quality: Guideline Technical Document – Manganese*. ((Catalogue No H144-39/2017E-PDF).). Ottawa, Ontario.: Health Canada

Canterford, J. H. (1985). Magnesia—An important Industrial Mineral: A Review of Processing Options and Uses. *Mineral Processing and Extractive Metallurgy Review, 2*(1-2), 57-104. doi:10.1080/08827508508952601

Cao, C.-Y., Qu, J., Wei, F., Liu, H., & Song, W.-G. (2012). Superb Adsorption Capacity and Mechanism of Flowerlike Magnesium Oxide Nanostructures for Lead and Cadmium Ions. *ACS Applied Materials & Interfaces, 4*(8), 4283-4287. doi:10.1021/am300972z

Caraballo, M. A., Rötting, T. S., Macías, F., Nieto, J. M., & Ayora, C. (2009). Field multi-step limestone and MgO passive system to treat acid mine drainage with high metal concentrations. *Applied Geochemistry, 24*(12), 2301-2311. doi:https://doi.org/10.1016/j.apgeochem.2009.09.007

Caraballo, M. A., Rötting, T. S., & Silva, V. (2010). Implementation of an MgO-based metal removal step in the passive treatment system of Shilbottle, UK: Column experiments. *Journal of Hazardous Materials, 181*(1), 923-930. doi:https://doi.org/10.1016/j.jhazmat.2010.05.100

Chilingar, G. V., Mourhatch, R., & Al-Qahtani, G. D. (2008). CHAPTER 6 - SCALING. In G. V. Chilingar, R. Mourhatch, & G. D. Al-Qahtani (Eds.), *The Fundamentals of Corrosion and Scaling for Petroleum & Environmental Engineers* (pp. 117-139): Gulf Publishing Company.

Choi, H., Woo, N. C., Jang, M., Cannon, F. S., & Snyder, S. A. (2014). Magnesium oxide impregnated polyurethane to remove high levels of manganese cations from water. *Separation and Purification Technology, 136*, 184-189. doi:https://doi.org/10.1016/j.seppur.2014.08.037

Chou, L., Garrels, R. M., & Wollast, R. (1989). Comparative study of the kinetics and mechanisms of dissolution of carbonate minerals. *Chemical Geology, 78*(3), 269-282. doi:https://doi.org/10.1016/0009-2541(89)90063-6

Claveau-Mallet, D., Courcelles, B., Pasquier, P., & Comeau, Y. (2017). Numerical simulations with the P-Hydroslag model to predict phosphorus removal by steel slag filters. *Water Research, 126*, 421-432. doi:https://doi.org/10.1016/j.watres.2017.09.032

Cortina, J.-L., Lagreca, I., De Pablo, J., Cama, J., & Ayora, C. (2003). Passive In Situ Remediation of Metal-Polluted Water with Caustic Magnesia: Evidence from Column Experiments. *Environmental Science & Technology, 37*(9), 1971-1977. doi:10.1021/es026018m

Courcelles, B., Modaressi-Farahmand-Razavi, A., Gouvenot, D., & Esnault-Filet, A. (2011). Influence of Precipitates on Hydraulic Performance of Permeable Reactive Barrier Filters. *International Journal of Geomechanics, 11*(2), 142-151. doi:10.1061/(ASCE)GM.1943-5622.0000098

de Repentigny, C., Courcelles, B., & Zagury, G. J. (2018). Spent MgO-carbon refractory bricks as a material for permeable reactive barriers to treat a nickel- and cobalt-contaminated groundwater. *Environmental Science and Pollution Research, 25*(23), 23205-23214. doi:10.1007/s11356-018-2414-3

De Repentigny, C., Zagury, G., & Courcelles, B. (2019). Modeling of the clogging in a MgO column used to treat a Ni- and Co-contaminated water and performance prediction for a centripetal radial column. *Chemosphere, 236*. doi:10.1016/j.chemosphere.2019.07.038

Dion, L.-A., Saint-Amour, D., Sauvé, S., Barbeau, B., Mergler, D., & Bouchard, M. F. (2018). Changes in water manganese levels and longitudinal assessment of intellectual function in children exposed through drinking water. *NeuroToxicology, 64*, 118-125. doi:https://doi.org/10.1016/j.neuro.2017.08.015

Dreybrodt, W., Lauckner, J., Zaihua, L., Svensson, U., & Buhmann, D. (1996). The kinetics of the reaction CO2 + H2O → H+ + HCO3− as one of the rate limiting steps for the dissolution of calcite in the system H2O□CO2□CaCO3. *Geochimica et Cosmochimica Acta, 60*(18), 3375-3381. doi:https://doi.org/10.1016/0016-7037(96)00181-0

Eisenlohr, L., Meteva, K., Gabrovšek, F., & Dreybrodt, W. (1999). The inhibiting action of intrinsic impurities in natural calcium carbonate minerals to their dissolution kinetics in aqueous H2O–CO2 solutions. *Geochimica et Cosmochimica Acta, 63*(7), 989-1001. doi:https://doi.org/10.1016/S0016-7037(98)00301-9

EPA, U. S. (2004). *Drinking Water Health Advisory for Manganese*. (EPA-822-R-04-003). Washington, DC

Eubank, W. R. (1951). Calcination Studies of Magnesium Oxides. *Journal of the American Ceramic Society, 34*(8), 225-229. doi:10.1111/j.1151-2916.1951.tb11644.x

Evans, R. L., & Clair, H. W. S. (1949). Carbonation of Aqueous Suspensions Containing Magnesium Oxides or Hydroxides. *Industrial & Engineering Chemistry, 41*(12), 2814-2817. doi:10.1021/ie50480a036

Fedorockova, A., & Raschman, P. (2008). Effects of pH and acid anions on the dissolution kinetics of MgO. *Chemical Engineering Journal, 143*(1-3), 265-272. doi:10.1016/j.cej.2008.04.029

Feitknecht, W., & Braun, H. (1967). Der Mechanismus der Hydratation von Magnesiumoxid mit Wasserdampf. *Helvetica Chimica Acta, 50*(7), 2040-2053. doi:10.1002/hlca.19670500738

Frost, M. T., Jones, M. H., Flann, R. C., Hart, R. L., Strode, P. R., J., U. A., & Tassios, S. (1990). Application of caustic calcined magnesia to effluent treatment. *Transactions of the Institutions of Mining and Metallurgy: Section C 99*, 117-124.

Fruhwirth, O., Herzog, G. W., Hollerer, I., & Rachetti, A. (1985). Dissolution and hydration kinetics of MgO. *Surface Technology, 24*(3), 301-317. doi:https://doi.org/10.1016/0376-4583(85)90080-9

Gambou-Bosca, A., & Bélanger, D. (2016). Electrochemical accessibility of porous submicron MnO2 spheres as active electrode materials for electrochemical capacitors. *Electrochimica Acta, 201*, 20-29. doi:https://doi.org/10.1016/j.electacta.2016.03.108

Ginocchio, J. C. (1985). Protection against corrosion in drinking water distribution systems. *Anti-Corrosion Methods and Materials, 32*(8), 14-16. doi:10.1108/eb020369

Glasson, D. R. (1963). Reactivity of lime and related oxides. IX. Hydration of magnesium oxide. *Journal of Applied Chemistry, 13*(3), 119-123. doi:10.1002/jctb.5010130304

Gorichev, I., & Kipriyanov, N. (1984). Regular Kinetic Features of the Dissolution of Metal Oxides in Acidic Media. *Russian Chemical Reviews, 53*, 1039. doi:10.1070/RC1984v053n11ABEH003139

Haddad, M., Ohkame, T., Bérubé, P. R., & Barbeau, B. (2018). Performance of thin-film composite hollow fiber nanofiltration for the removal of dissolved Mn, Fe and NOM from domestic groundwater supplies. *Water Research, 145*, 408-417. doi:https://doi.org/10.1016/j.watres.2018.08.032

Hasson, D., & Bendrihem, O. (2006). Modeling remineralization of desalinated water by limestone dissolution. *Desalination, 190*, 189-200. doi:10.1016/j.desal.2005.09.003

Hasson, D., Semiat, R., Shemer, H., Priel, M., & Nadav, N. (2013). Simple process for hardening desalinated water with Mg2+ ions. *Desalination and Water Treatment, 51*(4-6), 924-929. doi:10.1080/19443994.2012.707375

Health Canada. (2015). *Guidelines for Canadian Drinking Water Quality: Guideline Technical Document — pH*. (Catalogue No H144-28/2016E-PDF). Ottawa, Ontario: Health Canada

Hiortdahl, K. M., & Borden, R. C. (2014). Enhanced Reductive Dechlorination of Tetrachloroethene Dense Nonaqueous Phase Liquid with EVO and Mg(OH)2. *Environmental Science & Technology, 48*(1), 624-631. doi:10.1021/es4042379

Hövelmann, J., Putnis, C. V., & Benning, L. G. (2018). Metal Sequestration through Coupled Dissolution–Precipitation at the Brucite–Water Interface. *Minerals, 8*(8). doi:10.3390/min8080346

Huang, H.-H., & Liu, Q. (1995). Bench-Scale Chemical Treatability Study of the Berkeley Pit Water. In *Emerging Technologies in Hazardous Waste Management V* (Vol. 607, pp. 196-209): American Chemical Society.

Jägle, E. A., & Mittemeijer, E. J. (2011). The kinetics of grain-boundary nucleated phase transformations: Simulations and modelling. *Acta Materialia, 59*(14), 5775-5786. doi:https://doi.org/10.1016/j.actamat.2011.05.054

Jin, F., & Al-Tabbaa, A. (2014). Characterisation of different commercial reactive magnesia. *Advances in Cement Research, 26*(2), 101-113. doi:10.1680/adcr.13.00004

Johnson, W. A., & Mehl, R. F. (1939). Reaction kinetics in processes of nucleation and growth. *American Institute of Mining and Metallurgical Engineers -- Transactions, 135*, 416-442.

Jones, C. F., Segall, R. L., Smart, R. S. C., Turner, P. S., & Craig, D. P. (1981). Initial dissolution kinetics of ionic oxides. *Proceedings of the Royal Society of London. A. Mathematical and Physical Sciences, 374*(1756), 141-153. doi:10.1098/rspa.1981.0014

Jordan, G., Higgins, S., & Eggleston, C. (1999). Dissolution of the Periclase (001) Surface: A Scanning Force Microscope Study. *American Mineralogist, 84*. doi:10.2138/am-1999-1-216

Kameda, T., Takeuchi, H., & Yoshioka, T. (2009). Preparation of organic acid anion-modified magnesium hydroxides by coprecipitation: A novel material for the uptake of heavy metal ions from aqueous solutions. *Journal of Physics and Chemistry of Solids, 70*(7), 1104-1108. doi:https://doi.org/10.1016/j.jpcs.2009.06.006

Kameda, T., Yamamoto, Y., Kumagai, S., & Yoshioka, T. (2020). Effect of the specific surface area of MgO on the treatment of boron and fluorine. *Applied Water Science, 10*(5), 104. doi:10.1007/s13201-020-01198-z

Kato, Y., Yamashita, N., Kobayashi, K., & Yoshizawa, Y. (1996). Kinetic study of the hydration of magnesium oxide for a chemical heat pump. *Applied Thermal Engineering, 16*(11), 853-862. doi:https://doi.org/10.1016/1359-4311(96)00009-9

Kitamura, A., Onizuka, K., & Tanaka, K. (1996). Hydration Characteristics of Magnesia. *Taikabutsu Overseas, 16*(3), 3-11.

Kolmogorov, A. N. (1937). *On the Statistical Theory of the Crystallization of Metals*. Bulletin of the Academy of Sciences of the USSR, Mathematics Series

Langmuir, D. (1997). *Aqueous environmental geochemistry*. Upper Saddle River, N.J.: Prentice Hall.

Larson, T. E., Lane, R. W., & Neff, C. H. (1959). Stabilization of magnesium hydroxide in solids-contact process. *American Water Works Association -- Journal, 51*(12), 1551-1558.

Layden, G. K., & Brindley, G. W. (1963). Kinetics of Vapor-Phase Hydration of Magnesium Oxide. *Journal of the American Ceramic Society, 46*(11), 518-522. doi:10.1111/j.1151-2916.1963.tb14602.x

Letterman, R. D., Driscoll, C. T., Haddad, M., & Hsu, H. A. (1987). Limestone bed contactors for control of corrosion at small water utilities. *US EPA. Water Engineering Research Laboratory*.

Liu, B., Thomas, P. S., Ray, A. S., & Guerbois, J. P. (2007). ATG analysis of the effect of calcination conditions on the properties of reactive magnesia. *Journal of Thermal Analysis and Calorimetry, 88*(1), 145-149. doi:10.1007/s10973-006-8106-0

Liu, J. P., Wang, Y. J., Tian, Q., & Zhang, S. Z. (2012). Modeling hydration process of magnesia based on nucleation and growth theory: The isothermal calorimetry study. *Thermochimica Acta, 550*, 27-32. doi:10.1016/j.tca.2012.09.033

Liu, Z., Yuan, D., & Dreybrodt, W. (2005). Comparative study of dissolution rate-determining mechanisms of limestone and dolomite. *Environmental Geology, 49*(2), 274-279. doi:10.1007/s00254-005-0086-z

Ljung, K., & Vahter, M. (2007). Time to re-evaluate the guideline value for manganese in drinking water? *Environmental Health Perspectives, 115*(11), 1533-1538. doi:10.1289/ehp.10316

Luptáková, A., & Derco, J. (2015). Improving of drinking water quality by remineralisation. *Acta Chimica Slovenica; Vol 62, No 4 (2015)DO - 10.17344/acsi.2015.1590*. Retrieved from https://journals.matheo.si/index.php/ACSi/article/view/1590

Machel, H. G. (2005). SEDIMENTARY ROCKS | Dolomites. In R. C. Selley, L. R. M. Cocks, & I. R. Plimer (Eds.), *Encyclopedia of Geology* (pp. 79-94). Oxford: Elsevier.

Macías, F., Caraballo, M. A., Rötting, T. S., Pérez-López, R., Nieto, J. M., & Ayora, C. (2012). From highly polluted Zn-rich acid mine drainage to non-metallic waters: Implementation of a multi-step alkaline passive treatment system to remediate metal pollution. *Science of the Total Environment, 433*, 323-330. doi:https://doi.org/10.1016/j.scitotenv.2012.06.084

McGowan, W. (2000). *Water processing: residential, commercial, light-industrial* (3rd ed. ed.). Lisle, IL,: Water Quality Association.

Mejias, J. A., Berry, A. J., Refson, K., & Fraser, D. G. (1999). The kinetics and mechanism of MgO dissolution. *Chemical Physics Letters, 314*(5), 558-563. doi:https://doi.org/10.1016/S0009-2614(99)00909-4

Mo, L., Deng, M., & Tang, M. (2010). Effects of calcination condition on expansion property of MgO-type expansive agent used in cement-based materials. *Cement and Concrete Research, 40*(3), 437-446. doi:https://doi.org/10.1016/j.cemconres.2009.09.025

Monarca, S., Donato, F., Zerbini, I., Calderon, R. L., & Craun, G. F. (2006). Review of epidemiological studies on drinking water hardness and cardiovascular diseases. *European Journal of Cardiovascular Prevention & Rehabilitation, 13*(4), 495-506. doi:10.1097/01.hjr.0000214608.99113.5c

Morse, J. W., & Arvidson, R. S. (2002). The dissolution kinetics of major sedimentary carbonate minerals. *Earth-Science Reviews, 58*(1), 51-84. doi:https://doi.org/10.1016/S0012-8252(01)00083-6

Morse, J. W., Arvidson, R. S., & Lüttge, A. (2007). Calcium Carbonate Formation and Dissolution. *Chemical Reviews, 107*(2), 342-381. doi:10.1021/cr050358j

Navarro, A., Chimenos, J. M., Muntaner, D., & Fernández, A. I. (2006). Permeable Reactive Barriers for the Removal of Heavy Metals: Lab-Scale Experiments with Low-Grade Magnesium Oxide. *Groundwater Monitoring & Remediation, 26*(4), 142-152. doi:10.1111/j.1745-6592.2006.00118.x

Nield, D. A., & Bejan, A. (2017). *Convection in Porous Media* (5 ed.): Springer International Publishing.

Oulhote, Y., Mergler, D., Barbeau, B., Bellinger, D. C., Bouffard, T., Brodeur, M.-È., . . . Bouchard, M. F. (2014). Neurobehavioral Function in School-Age Children Exposed to Manganese in Drinking Water. *122*(12), 1343-1350. doi:doi:10.1289/ehp.1307918

Oustadakis, P., Agatzini-Leonardou, S., & Tsakiridis, P. E. (2006). Nickel and cobalt precipitation from sulphate leach liquor using MgO pulp as neutralizing agent. *Minerals Engineering, 19*(11), 1204-1211. doi:https://doi.org/10.1016/j.mineng.2005.11.006

Pishtshev, A., Karazhanov, S. Z., & Klopov, M. (2014). Materials properties of magnesium and calcium hydroxides from first-principles calculations. *Computational Materials Science, 95*, 693-705. doi:https://doi.org/10.1016/j.commatsci.2014.07.007

Plummer, L. N., Parkhurst, D. L., & Wigley, T. M. L. (1979). Critical Review of the Kinetics of Calcite Dissolution and Precipitation. In *Chemical Modeling in Aqueous Systems* (Vol. 93, pp. 537-573): AMERICAN CHEMICAL SOCIETY.

Plummer, L. N., Wigley, T. M. L., & Parkhurst, D. L. (1978). The kinetics of calcite dissolution in CO 2 -water systems at 5 degrees to 60 degrees C and 0.0 to 1.0 atm CO 2. *American Journal of Science, 278*(2), 179-216. Retrieved from http://www.ajsonline.org/content/278/2/179.short

Pokrovsky, O. S., Schott, J., & Castillo, A. (2005). Kinetics of brucite dissolution at 25°C in the presence of organic and inorganic ligands and divalent metals. *Geochimica et Cosmochimica Acta, 69*(4), 905-918. doi:https://doi.org/10.1016/j.gca.2004.08.011

Post, J. E. (1999). Manganese oxide minerals: Crystal structures and economic and environmental significance. *Proceedings of the National Academy of Sciences, 96*(7), 3447. doi:10.1073/pnas.96.7.3447

Pourahmad, H., Haddad, M., Claveau-Mallet, D., & Barbeau, B. (2019). Impact of media coating on simultaneous manganese removal and remineralization of soft water via calcite contactor. *Water Research, 161*, 601-609. doi:https://doi.org/10.1016/j.watres.2019.06.037

Rocha, S. D. F., Mansur, M. B., & Ciminelli, V. S. T. (2004). Kinetics and mechanistic analysis of caustic magnesia hydration. *Journal of Chemical Technology & Biotechnology, 79*(8), 816-821. doi:10.1002/jctb.1038

Ropp, R. C. (2013). Chapter 3 - Group 16 (O, S, Se, Te) Alkaline Earth Compounds. In R. C. Ropp (Ed.), *Encyclopedia of the Alkaline Earth Compounds* (pp. 105-197). Amsterdam: Elsevier.

Rötting, T. S., Ayora, C., & Carrera, J. (2008). Improved Passive Treatment of High Zn and Mn Concentrations Using Caustic Magnesia (MgO): Particle Size Effects. *Environmental Science & Technology, 42*(24), 9370-9377. doi:10.1021/es801761a

Rötting, T. S., Cama, J., Ayora, C., Cortina, J.-L., & De Pablo, J. (2006). Use of Caustic Magnesia To Remove Cadmium, Nickel, and Cobalt from Water in Passive Treatment Systems: Column Experiments. *Environmental Science & Technology, 40*(20), 6438-6443. doi:10.1021/es061092g

Schiller, J. E., Tallman, D. N., & Khalafalla, S. E. (1984). Mineral processing water treatment using magnesium oxide. *Environmental Progress, 3*(2), 136-141. doi:10.1002/ep.670030216

Schwartz, R., Shemer, H., Hasson, D., & Semiat, R. (2015). Design model for magnesium ions re-mineralization of desalinated water by dissolution of magnesia pellets. *Desalination, 373*, 10-15. doi:https://doi.org/10.1016/j.desal.2015.06.024

Segall, R. L., Smart, R. S. C., & Turner, P. S. (1978). Ionic oxides: distinction between mechanisms and surface roughening effects in the dissolution of magnesium oxide.

Journal of the Chemical Society, Faraday Transactions 1: Physical Chemistry in Condensed Phases, 74(0), 2907-2912. doi:10.1039/F19787402907

Shand, M. A. (2006a). Physical and Chemical Properties of Magnesium Oxide. In *The Chemistry and Technology of Magnesia* (pp. 121-131): Wiley Online Books.

Shand, M. A. (2006b). Water and Wastewater Applications for Magnesia Products. In *The Chemistry and Technology of Magnesia* (pp. 155-177).

Shemer, H., Hasson, D., & Semiat, R. (2015). State-of-the-art review on post-treatment technologies. *Desalination, 356*, 285-293. doi:https://doi.org/10.1016/j.desal.2014.09.035

Skousen, J., Zipper, C. E., Rose, A., Ziemkiewicz, P. F., Nairn, R., McDonald, L. M., & Kleinmann, R. L. (2017). Review of Passive Systems for Acid Mine Drainage Treatment. *Mine Water and the Environment, 36*(1), 133-153. doi:10.1007/s10230-016-0417-1

Sly, L., Hodgkinson, M., & Arunpairojana, V. (1990). Deposition of manganese in a drinking water system. *Applied and Environmental Microbiology, 56*, 628-639. doi:10.1128/AEM.56.3.628-639.1990

Smithson, G. L., & Bakhshi, N. N. (1969). The kinetics and mechanism of the hydration of magnesium oxide in a batch reactor. *The Canadian Journal of Chemical Engineering, 47*(6), 508-513. doi:10.1002/cjce.5450470602

Stokes, P. M., Campbell, P. G. C., Schroeder, W. H., Trick, C., France, R. L., Pockett, K. J., Lazertz, B., Speyer, H., Hanna, J. E., and Donaldson, J. (1988). *Manganese in the Canadian Environment*.

Stumm, W. (1997). Reactivity at the mineral-water interface: dissolution and inhibition. *Colloids and Surfaces A: Physicochemical and Engineering Aspects, 120*(1), 143-166. doi:https://doi.org/10.1016/S0927-7757(96)03866-6

Stumm, W., & Morgan, J. J. (1996). *Aquatic chemistry : chemical equilibria and rates in natural waters*. New York: Wiley.

Svensson, U., & Dreybrodt, W. (1992). Dissolution kinetics of natural calcite minerals in CO2-water systems approaching calcite equilibrium. *Chemical Geology, 100*(1), 129-145. doi:https://doi.org/10.1016/0009-2541(92)90106-F

Tang, X., Guo, L., Chen, C., Liu, Q., Li, T., & Zhu, Y. (2014). The analysis of magnesium oxide hydration in three-phase reaction system. *Journal of Solid State Chemistry, 213*, 32-37. doi:https://doi.org/10.1016/j.jssc.2014.01.036

Teringo Iii, J. (1987). Magnesium hydroxide reduces sludge/improves filtering. *Pollution Engineering, 19*(4), 78-83.

Thomas, J. J. (2007). A New Approach to Modeling the Nucleation and Growth Kinetics of Tricalcium Silicate Hydration. *Journal of the American Ceramic Society, 90*(10), 3282-3288. doi:10.1111/j.1551-2916.2007.01858.x

Thomas, J. J., Musso, S., & Prestini, I. (2014). Kinetics and Activation Energy of Magnesium Oxide Hydration. *Journal of the American Ceramic Society, 97*(1), 275-282. doi:10.1111/jace.12661

Vermilyea, D. A. (1969). The Dissolution of MgO and Mg(OH)[sub 2] in Aqueous Solutions. *Journal of the Electrochemical Society, 116*(9), 1179. doi:10.1149/1.2412273

Voutchkov, N. (2012). *Desalination Engineering - Planning and Design, McGraw Hill, 2012*.

Wasserman, G. A., Liu, X., Parvez, F., Ahsan, H., Levy, D., Factor-Litvak, P., . . . Graziano, J. H. (2006). Water manganese exposure and children's intellectual function in Araihazar, Bangladesh. *Environ Health Perspect, 114*(1), 124-129. doi:10.1289/ehp.8030

Withers, A. (2005). Options for recarbonation, remineralisation and disinfection for desalination plants. *Desalination, 179*(1), 11-24. doi:https://doi.org/10.1016/j.desal.2004.11.051

Wogelius, R. A., Refson, K., Fraser, D. G., Grime, G. W., & Goff, J. P. (1995). Periclase surface hydroxylation during dissolution. *Geochimica et Cosmochimica Acta, 59*(9), 1875-1881. doi:https://doi.org/10.1016/0016-7037(95)00070-G

World Health, O. (2009). Calcium and magnesium in drinking-water, Public health significance.

World Health, O. (2017). *Guidelines for drinking-water quality: fourth edition incorporating first addendum* (4th ed + 1st add ed.). Geneva: World Health Organization.

World Health Organisation (WHO). (2005). Nutrients in drinking water. In. Geneva.

Yamauchi, V., Tanaka, K., Hattori, K., Kondo, M., & Ukawa, N. (1987). Remineralization of desalinated water by limestone dissolution filter. *Desalination, 66*, 365-383. doi:https://doi.org/10.1016/0011-9164(87)90218-9

Younger, P., Banwart, S., & Hedin, R. (2002). Mine water, Hidrology, Pollution, Remediation. *Environmental Pollution, 5*.

APPENDIX B MEDIA CHARACTERIZATION

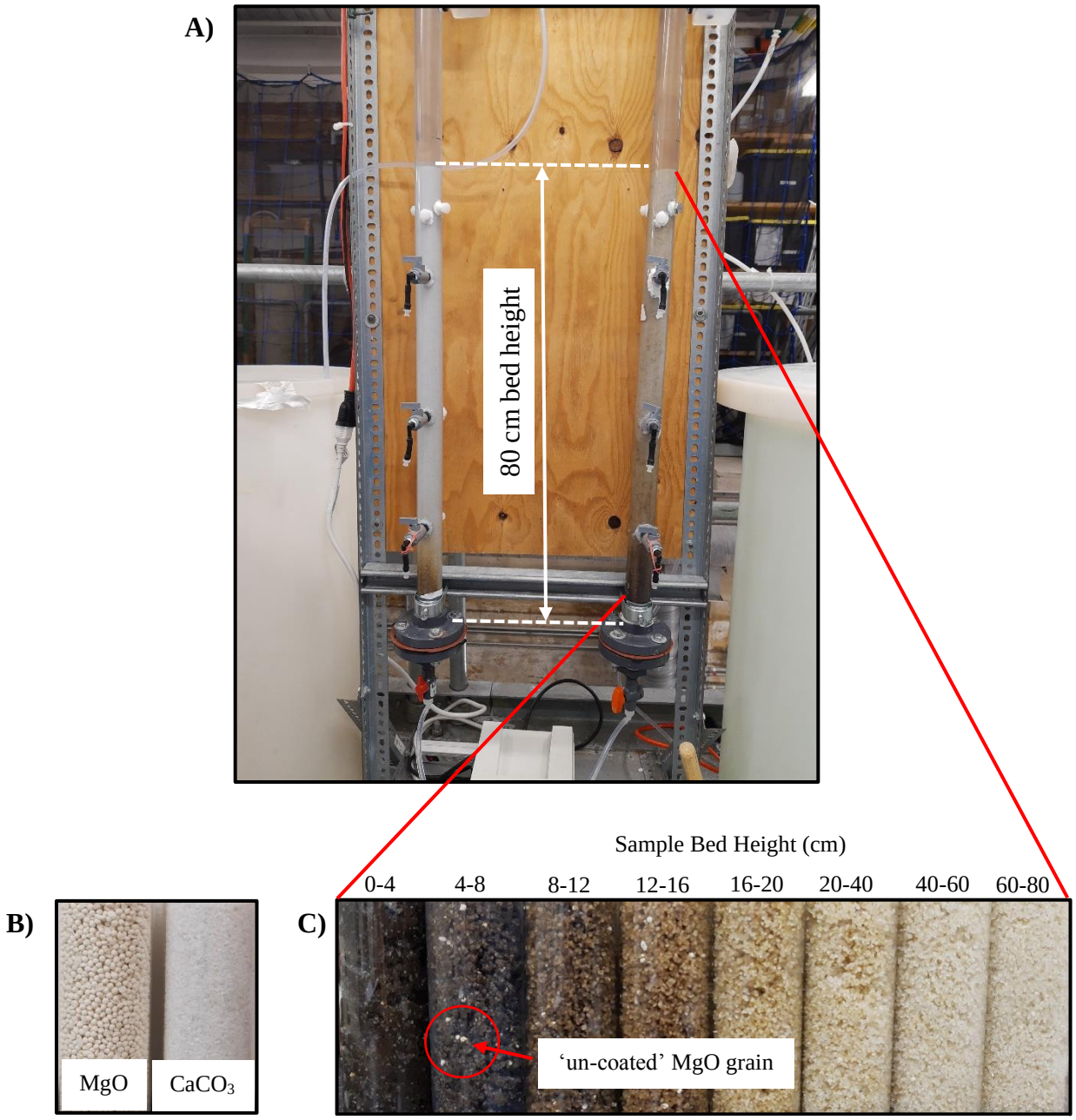

Figure A.1 A) Mixed media columns containing 5% MgO after 720 hours of operation, B) fresh MgO and $CaCO_3$ and C) used media samples taken from column B after treating 5 mg Mn/L for 30 days. The red circle shows MgO grains that do not visibly appear to be coated with solid Mn-phase (MnO_x).